Two-Dimensional Mathematical Analysis of the Faraday Cage

Michael Lyons

July 23, 2018

MA960 Dissertation
Email Address: mpl21@kent.ac.uk
Supervisor: Steffen Krusch

Abstract

A Faraday cage is a non-continuous enclosure formed from a conductive material that is capable of blocking electromagnetic fields either partially or completely. Mathematical analysis of this particular scientific phenomena is surprisingly lacking and as such we attempt to further the exploration of this subject in some small way.

This dissertation focuses on the content of an article titled "Mathematics of the Faraday Cage" by Chapman, Hewett and Trefethen and seeks to extend a model produced by these authors to a variety of different circumstances. Included also is material expanding on an explanation of the model itself as well as other relevant details.

We focus on answering questions such as, what are the effects of changing the shape of the Faraday cage? Do two Faraday cages produce greater effects than one? How do we need to adapt the shape of the Faraday cage in order to best protect a given shape?

Some attention is also paid to possibilities in regards to extending our model to three-dimensions as well as potential practical applications.

Contents

1 Introduction

Electromagnetism exists as one of the four fundamental forces that define how the world around us functions. By developing our understanding of this force we are able to make progress as a species in our goal of better understanding the world around us and develop a more refined idea of how the universe operates. Quite naturally this subject has managed to capture the attention and fascination of countless scores of people, particularly when it became clear that electricity and magnetism were strongly linked in the first half of the nineteenth century. Amongst these people there have of course been mathematicians, people who have sought to utilise numerical methods to dive to the heart of just how electromagnetism functions in as true and comprehensive a sense as we can. It is thanks to these people that our understanding of the subject has reached the point it has today. Despite the history and the attention that has been devoted to this subject there will of course inevitably be areas of it that demand further attention, one such area being the mathematics of the Faraday cage. This subject has seen some exploration though not in great depth, for example this not be a topic that would appear in mathematical textbooks. This means that there is still work to be done and questions to be answered if we wish to propel our understanding of this topic forwards. Now to begin, what exactly is a Faraday cage?

Suppose that we have an area or perhaps an object that we wish to shield from electromagnetic radiation. This might be a sensitive piece of electronic equipment, or it might even be a person. A natural solution would be to use a conductive material capable of blocking electromagnetic waves, and form it into a continuous covering. This would effectively shield the object from the waves, in the case of electronics preventing their functioning from being disrupted, or in the case of a person perhaps protecting them from dangerous X-rays. This continuous conductive covering could be described as a Faraday shield. To give a concrete example we can consider an electrical cable such as the one shown in figure 1, where a Faraday shield is used to ensure the data being transmitted through the cable is not disrupted.

Suppose however that we have this same goal in mind but have an additional condition attached to our problem, that we wish to minimise the amount of material used whilst still maintaining at a minimum some specified level of shielding. If we were to use a metal mesh rather than a continuous sheet we would quickly find that whilst there is a reduction in the shielding provided the results obtained are still at an acceptable level. This is an interesting scientific phenomenon and will be explored in depth over the course of this dissertation. We would call this mesh covering a Faraday cage.

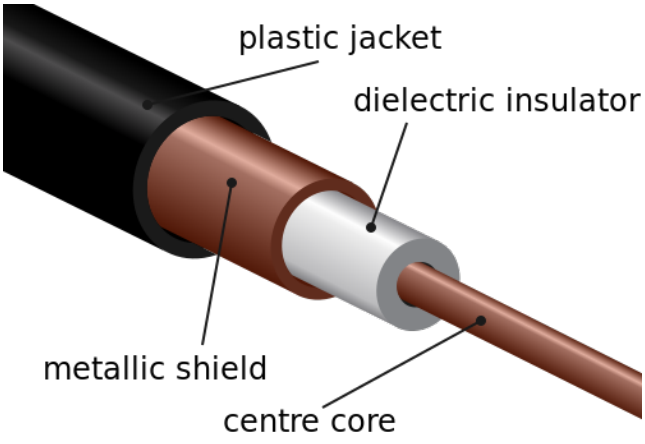

Figure 1: A practical application of a Faraday shield, here a layer of metal contained within the jacket is used to block outside sources of electromagnetic radiation, preventing the data being transmitted through the wire from being disrupted.

Figure 2: A practical application of a Faraday cage, here a metal mesh is used to provide electromagnetic shielding at a power plant.

We can distil these ideas down into the form of two simple definitions.

Definition 1. A Faraday shield is defined as an enclosure formed from a continuous conductive material that is capable of providing electromagnetic shielding.

Definition 2. A Faraday cage is defined as an enclosure formed from a conductive mesh that is capable of providing electromagnetic shielding.

The Faraday cage was first discovered in 1839 by Michael Faraday as part of his experiments involving electricity, forming a part of his body of work that helped electricity become a viable technology. In "Experimental Researches in Electricity" [2], Faraday records the following observation

"I put a delicate gold-leaf electrometer within the cube, and then charged the whole by an outside communication, very strongly, for some time together; but neither during the charge or after the discharge did the electrometer or air within show the least signs of electricity."

The situation Faraday outlines here is fairly simple as there is near perfect shielding which depends only upon the thickness of the material used to form the shield. If instead of a Faraday shield we use a Faraday cage the situation becomes more complicated. As the mesh becomes thinner the proportion of the electromagnetic field that penetrates increases but this relationship is by no means simple, as we shall soon see.

Despite the Faraday cage being a well known scientific phenomenon even amongst the general public, it has seen surprisingly little exploration in a mathematical context. One of the few existing explorations of the topic may be found in "The Feynman Lectures on Physics" [3] in section 7-5. This analysis has since been proven to be flawed in its approach, Feynman coming to the conclusion that the strength of the effect is exponential in nature. This error arises due to Feynman considering equal charges rather than equal potentials, the lack of the presence of an external field, and the wires being considered to have infinitesimal radius.

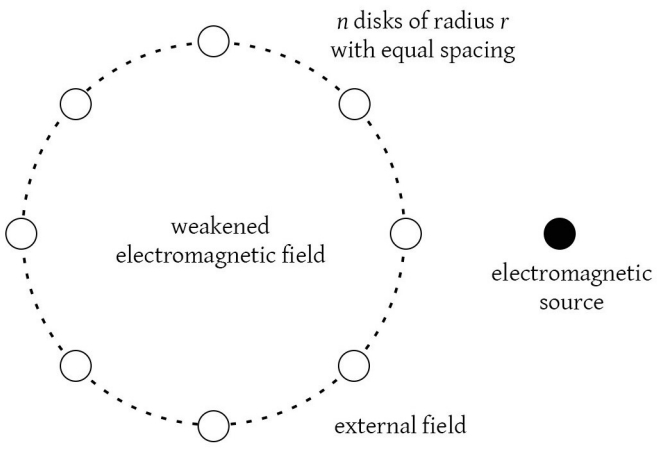

Figure 3: A Faraday cage comprised of 8 disks placed along the boundary of a circle.

Where Feynman considered the character of the electric field near an infinitely long grid of charged wires we will instead for the most part be looking at a situation involving a single cage comprised of disks placed along the boundary of a circle or a regular polygon. This general situation can be seen in figure 3. Put simply we have the our cage, as well as an electromagnetic source located outside of this cage and we wish to measure the effectiveness of the shielding provided by this cage. Our initial means of doing this will be by measuring the strength of the electric field at the center of the cage however we will explore alternate approaches at a later point.

MATLAB will be used throughout the course of this dissertation to relevant data and allow us to produce visual representations of this data. Details on the model used are provided in section 2 whilst samples of the code used as well as explanations on the nature of this code are provided in appendices A and B.

This dissertation is strongly center around an article titled "Mathematics of the Faraday Cage" [1] authored by Chapman, Hewett, and Trefethen, with our main goal being to provide additional details regarding the formulation of a model produced in this article and to extend this model into a variety of different circumstances.

In [1] the authors provide three different models as well as a selection of results obtained using these models. We will be primarily concerned with the first of these three models, the two-dimensional electrostatic model. For this model we will cover the formulation and necessary information in detail as well as providing additional clarifying detail. Once we have done this we will move onto the bulk of the material presented which will consist of using our model and adapting it in various ways to make conclusions about a number of different questions. For example we may wish to ask, what are the effects of changing the shape of the Faraday cage? Do two Faraday cages produce greater effects than one? How do we need to adapt the shape of the Faraday cage in order to best protect a given shape?

We will also be attempting to match results obtained to real-life problems, considering how models like the one we will be considering may be used to provide a tangible benefit and how they might be used in practice. Keeping this in mind we proceed to move into a formal mathematical context and begin our analysis of the general situation surrounding the Faraday cage.

2 The Formulation of our Model

2.1 Maxwell's Equations

The basis of the model we will be considering originates in Maxwell's equations, so let us first cover these equations briefly before moving onto the formulation of the model itself.

Maxwell's equations take their name from notable mathematician James Maxwell who took a set of previously known laws and condensed them down into a symmetric set of equations. These equations are laws, fundamental and universal rules that govern the behaviour of electromagnetic fields. As we are working with Faraday cages, objects that serve the purpose of blocking electromagnetic waves, it is only natural that we use these basic equations as our starting point.

Maxwell's equations are as follows:

$$\nabla \cdot D = \rho_v \tag{1}$$

$$\nabla \cdot B = 0 \tag{2}$$

$$\nabla \times E = -\frac{\partial B}{\partial t} \tag{3}$$

$$\nabla \times H = J + \frac{\partial D}{\partial t} \tag{4}$$

To properly understand these equations we first need to cover two key definitions.

Definition 3. Divergence at a point (x,y,z) is the measure of the vector flow out of a surface surrounding that point. The divergence operator is denoted $\nabla\cdot$ and is defined mathematically for D as:

$$\nabla \cdot D = \frac{\partial D_x}{\partial x} + \frac{\partial D_y}{\partial y} + \frac{\partial D_z}{\partial z}$$

We can think of this concept in simple terms, if the divergence is positive then this means that the point is a source, if it is negative then this means that the point is a sink. It can be said that the divergence is a measure of how fields flow away from a point.

Definition 4. The curl of E is defined mathematically to be:

$$\nabla \times E = \Big\{\frac{\partial E_z}{\partial y} - \frac{\partial E_y}{\partial z}\Big\}\hat{x} + \Big\{\frac{\partial E_x}{\partial z} - \frac{\partial E_z}{\partial x}\Big\}\hat{y} + \Big\{\frac{\partial E_y}{\partial x} - \frac{\partial E_x}{\partial y}\Big\}\hat{z}$$

The curl is difficult to define in a simple fashion, though if we consider the divergence to be a measure of how fields flow away from a point then we say that the curl is a measure of how fields wrap around a point. The curl operates on a vector function and returns a vector function, the resulting vector function being a measure of the rotation of the field.

Now that we have defined both of these two terms we can cover what exactly these equations mean.

Equation (1) is known as Gauss' Law, which dictates how an electric field behaves around electric charges. This is simply a formalisation of a simple idea, that like charges repel each other whilst opposites attract. Linking this to equation itself we have that $\nabla \cdot D$, the divergence of the electric flux density, is equal to the volume charge density, ρ_v.

Equation (2) is known as Gauss' Magnetism Law and states that the divergence of the magnetic flux density $\nabla \cdot B$, is equal to zero. The major consequence of this is that magnetic monopoles cannot exist.

Equation (3) is known as Faraday's law, stating that the curl of the electric field is equal to the rate of change of the magnetic field over time. A natural consequence of this is that electric current gives rise to magnetic fields and that magnetic fields give rise to electric current.

Equation (4) is known as Ampere's Law which states that the curl of the magnetic field is equal to the rate of change of the electric field over time added to the electric current density, J.

Now we have these equations we need to consider the case we are interested in and produce the equations that are relevant to our situation. We are specifically dealing with the electrostatic case and as such Maxwell's equations may be reduced down to the following two equations:

$$\nabla \cdot E = -\frac{\rho(x)}{\epsilon_0} \tag{5}$$

$$\nabla \times E = 0 \tag{6}$$

Making use of Helmholtz's theorem we can specify the charge density and then as we know the divergence and curl of the vector field if we also have the boundary conditions then we can uniquely determine the electromagnetic field everywhere within the boundary.

If we then write equations (5) and (6) in terms of the potential equation (6) vanishes whilst equation (5) becomes

$$\nabla^2 V = -\frac{1}{\epsilon_0}\rho(x), \tag{7}$$

which is known as the Poisson equation.

We can further reduce this down to the Laplace equation

$$\nabla^2 V = 0, \tag{8}$$

as there are no sources in our region, $\rho(x) = 0$.

To progress further we need to consider the specifics of our situation and the exact conditions we will be working with.

2.2 Defining the Situation

Given a bounded simply connected open subset of the plane with boundary Γ, suppose that we place n disks of radius r along Γ with a fixed distance between neighbouring disk centres. We can take Γ to be say a regular polygon as in figure 2, or we could use a Γ with a less regular shape, for example we could use a Γ that is a two dimensional approximation of a microwave, as in figure 3.

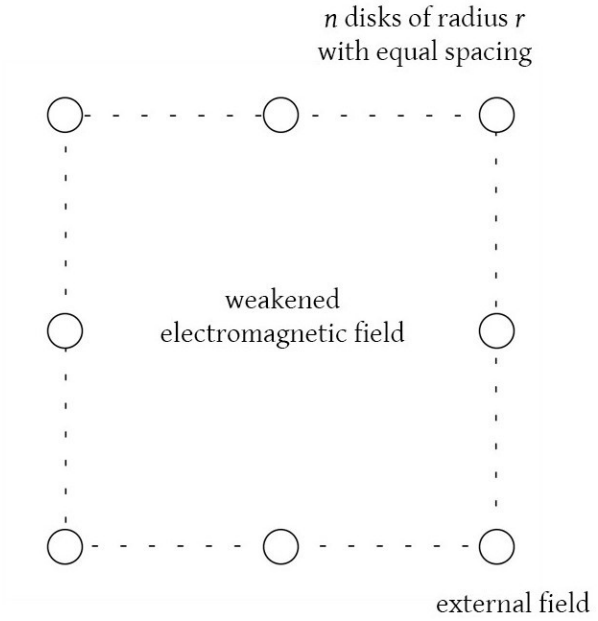

Figure 4: A Faraday cage with a boundary in the shape of a square.

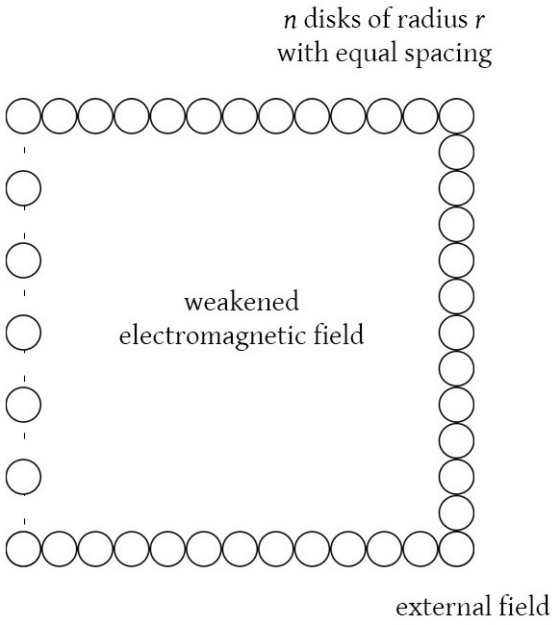

Figure 5: A Faraday cage in the shape of a two-dimensional approximation of a microwave oven.

The exact nature of the configuration that we will use will change throughout the course of the dissertation depending on the particular problem we are tackling. Typically we will use a regular polygon of some description, or a circle which we will consider to be a polygon with 360 sides.

We also note that we will be choosing to identify the complex z-plane with the x-y plane to simplify the formulation of the MATLAB code used. This does not affect the results obtained and is purely for the sake of convenience.

We seek a real function that satisfies the Laplace equation in the region of the plane that comprises the exterior of the disks. We also impose the boundary condition

$$\phi = \phi_0 \tag{9}$$

on the disks themselves.

These two equations are common ones when dealing the electromagnetic waves as they can be used to model the behaviour of electromagnetic potentials. This method as put forward by reference [1] is distinct in that it models the wires that comprise the disks as having a finite radius rather than an infinitesimal radius, such as in reference [2], meaning that they are not considered to be equal point charges.
This comes from the fact that ϕ_0 is a constant to be determined as part of the solution to the problem.

It is necessary that we specify an external source of electromagnetic radiation and that we use appropriate boundary conditions at infinity. We will be using a point charge of strength 2π located at a fixed point $z = z_s$ located outside of the boundary Γ. In the cases I will be covering this will also generally be the case, however I will also be analysing the situation in which our external source is located inside of the cage, as well as several situations in which this source is in a non-standard configuration. We stipulate that

$$\phi(z) = \log(|z - z_s|) + O(1) \text{ as } z \to z_s \tag{10}$$

and also that

$$\phi(z) = \log(|z|) + 0(1) \text{ as } z \to \infty. \tag{11}$$

The second of these two equations indicates that the total charge on the disks is equal to zero, however the charge on each of the disks individually will generally not be equal to zero.

Now that we have our problem established we can analyse potential methods of finding solutions. In [1] three different approaches are mentioned, as previously stated. These three methods are as follows: direct numerical calculation, an analytical bound based on conformal mapping, and a homogenised approximation derived from the method of multiple scales.

The first of these approaches, direct numerical calculation, I found the easiest to adapt and implement in MATLAB as the authors of the paper kindly provided a basic example of the code they were using. From this basic case, I could then make my own alterations as needed to test the various scenarios I wished to analyse. To begin we start by covering this approach in a purely mathematical sense and in the next section we will proceed to cover how it may be applied to problems.

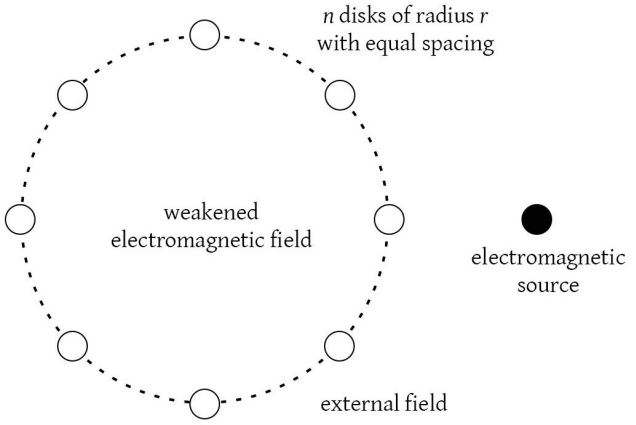

Figure 6: Our familiar Faraday cage example.

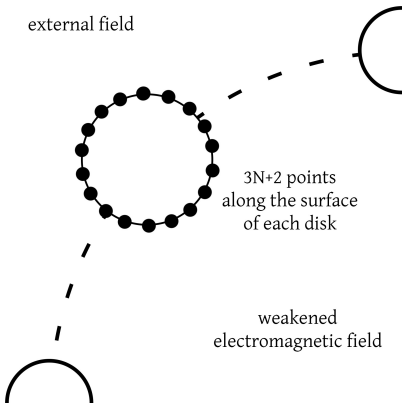

Figure 7: Discretising a disk into a number of individual points.

This problem can be solved through direct numerical calculation by the method of expansion in fundamental solutions of the Laplace equation through least-squares matching on the boundary. This method is often known as Miklhin's method and will be covered on the following page.

To begin we define the relevant terms. We define $\{c_j\}$ to be the center of the wires, each with a radius of r, and z to be a point in our model with $\{z_s\}$ being the location of the point charge itself.
Now we make use of the following expansion

$$u(z) = \log|z - z_s| + \sum_{j=1}^{\infty} d_j \log|z - c_j| + Re\Big[\sum_{k=1}^{N}(a_{jk} - ib_{jk})(z - z_j)^{-k}\Big], \tag{12}$$

where $\{d_j\}, \{a_{jk}\}$, and $\{b_{jk}\}$ are real constants to be determined along with ϕ_0, which represents the constant voltage in the wires that form the cage.

We fix d_1 by applying the condition $\sum d_j = 0$, this is the condition of equation 11. Equation 12 satisfies equations 8,10, and 11 for any values of the coefficients, the aim is to have it also satisfy 9. This can be done be discretising the boundary of each disk into a number of points, we use $3N + 2$, this allows us to have equation 9 take the form of an overdetermined system of linear equations. This system of equations can then be easily solved by MATLAB using the backslash command. A typical output produced from the code we use can be seen in figures 8 and 9 below.

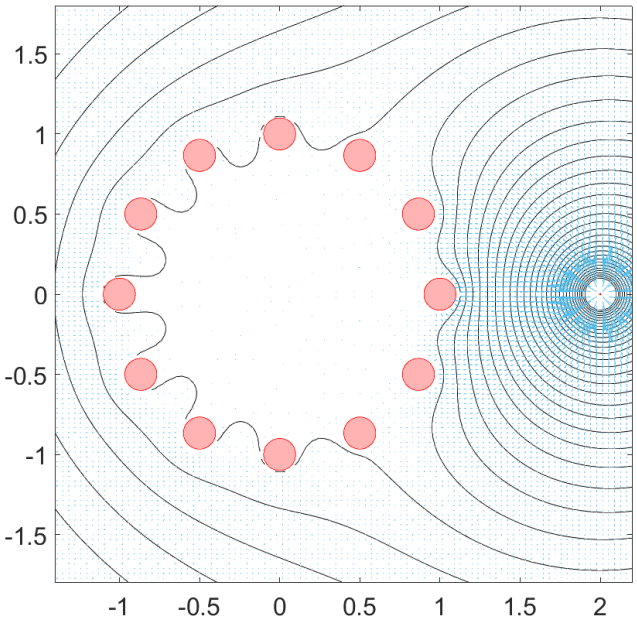

Figure 8: An example plot of the solution to equation 12, formulated using MATLAB. A quiver plot has been overlaid on top of the output to give a clear impression of the behaviour of the electromagnetic waves.

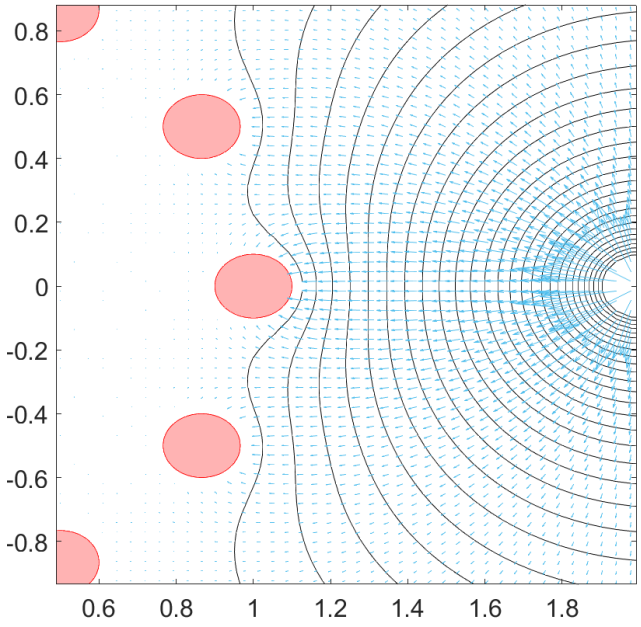

Figure 9: A zoomed in portion of figure 8. Note the disparity between the electromagnetic field strength inside and outside of the cage, the electromagnetic field is strongest near the source and is then diverted around the cage.

Finally, we make note of a value

$$\|\nabla\phi(0)\|, \tag{13}$$

which will be particularly useful moving forwards. This is the value of the strength of the electromagnetic field at the center of the cage and as such we will be using it as a means of comparison between different configurations of cages. A lower value would indicate a more successful arrangement for our cage.

3 Analysis of Simplistic Configurations

3.1 Initial Configuration

Now that we have an understanding of the methodology we are making use of we can begin applying it to specific problems and analyse the results obtained. To begin with we attempt to replicate the results obtained by the authors of [1].

The problem outlined in [1] is that of a a cage with a circular boundary, with disks placed such that every disk is an equal distance away from both of its neighbours, with a source placed a fixed distance away from the center of the cage. This basic configuration can be seen in figure 10.

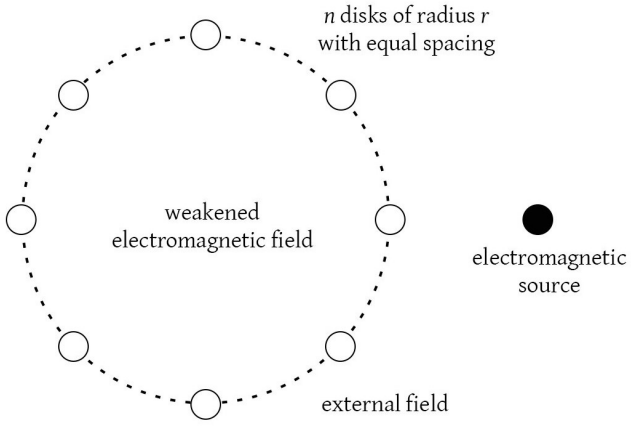

Figure 10: Our initial test problem.

As a means of analysing our results we are going to be making use of the value of $\|\nabla\phi(0)\|$ as previously stated.
This value is defined as the absolute value of the gradient of the electromagnetic field at the centre of the disk. This is the strength of the electromagnetic field at the center of the disk, in the absence of a cage this would take the value 0.5. The purpose of a Faraday cage is to shield the interior of the cage from electromagnetic radiation, as such we are primarily interested in minimizing this value, however there will be a case in section 5 in which we have a different aim.
It is worth thinking about how this means of comparison may be adjusted to suit a particular aim, for example we may be interested in minimising this value not just at the centre of the cage, but for the entire area contained within the cage on average.

Various questions may come to mind at this point. What is the effect of changing the number of disks? What is the effect of changing the radius of the wires? By making use of the code provided in Appendix A we can quite quickly produce results that match those found in [1].

Table 1: Varying number of disks and radius of wires for our initial test problem.

	r = 10^(-1)	10^(-2)	10^(-3)	10^(-4)	10^(-5)	10^(-6)
n = 5	0.1118	0.2663	0.3348	0.3723	0.3959	0.4121
10	0.0236	0.1582	0.2398	0.2901	0.3241	0.3486
20	0.0003	0.0698	0.1406	0.1916	0.2299	0.2598
40	0	0.0229	0.0693	0.1081	0.1405	0.1680
80	0	0.0047	0.0297	0.0538	0.0756	0.0954
160	0	0	0.0112	0.0246	0.0372	0.0492
320	0	0	0.0036	0.0105	0.0173	0.0239

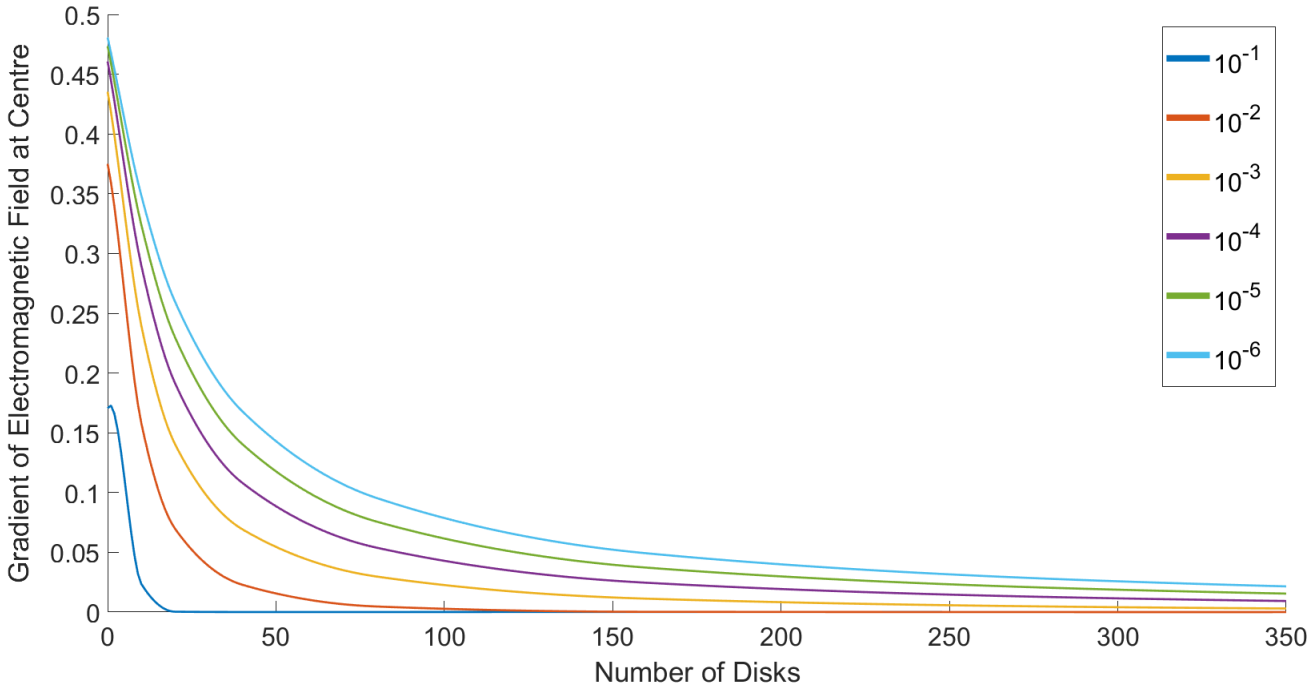

Figure 11: Plot displaying the effects of changing wire radius and the number of disks for a circular Faraday cage.

We can observe some general trends forming from these results. Firstly shielding improves as we increase the number of disks that comprise our cage, and as we increase the thickness of the wires used. It appears to be the case that the number of disks is a more important factor than the radius of the wires, even when the radius of the wires becomes very small we can still observe significant differences in the electromagnetic gradient at the centre. This would suggest that if we were to say, try and optimise our shielding whilst minimising the amount of material used, it may be in our best interests to use more disks and decrease the radius of each wire. Further attention will be given to this idea in a later section.

To put these results in a more intuitive form we can produce a simple plot using the data from the above table, which can be seen on the following page. It is worth noting that once we reach a wire thickness of around 10^{-3} we require a very large number of disks to reduce the value of $\|\nabla\phi(0)\|$ to zero, effective to four decimal places.

When we change various factors in regards to our configuration in the future we should expect that these core patterns should continue to occur, that increasing the number disks or the radius of the wires will result in a general decrease in the strength of the electromagnetic field within the confines of the cage. We can also use the results obtained here to formulate in our minds a general idea of the results we should expect in future, if we find our model outputting values that differ significantly from those found here that could possibly indicate an error in the model itself or our approach. These are of course assumptions that will need to be verified with time, however they provide a good starting point for our analysis.

In reference [1] the conclusion is reached that strength of the shielding effect is linear in n, logarithmic in r, and linear in $|z_s|$. They also produce a formula given specific conditions and verify their results with a theorem and a homogenised analysis.

We can now move forwards from this baseline set of results and onto more complicated situations.

3.2 The Effects of Changing the Shape of the Cage

Now that we have obtained a set of results for a simple case, that of a circular boundary, we can begin to attempt to generalise the situation further to increase the applicability of the results we obtain. For example, we may wish to move from our circular boundary to any n-sided polygon of our choosing.

We obtain results in a similar fashion to our previous case, however now we choose a fixed radius (0.1mm) and vary the number of disks that comprise the boundary as well the shape of the boundary. Here we will simply use a triangle, square, and circle. The results obtained can be seen in table 2.

Table 2: Varying number of disks and the number of sides forming the boundary.

	Triangle	Square	Circle
n = 5	0.0970	0.1009	0.1118
10	0.0109	0.0175	0.0236
20	0	0	0.0003
40	0	0	0

These results run contrary to what one might expect, the triangle apparently proving to superior in regards to the criteria we have put forth. The reason for this may be due to a factor that is not being controlled when we change the shape of the boundary, the surface area contained within the boundary. Reducing the surface area within the cage whilst using the same amount of material to compose the boundary would naturally lead to a reduction in the strength of the electromagnetic field at the center of the boundary.

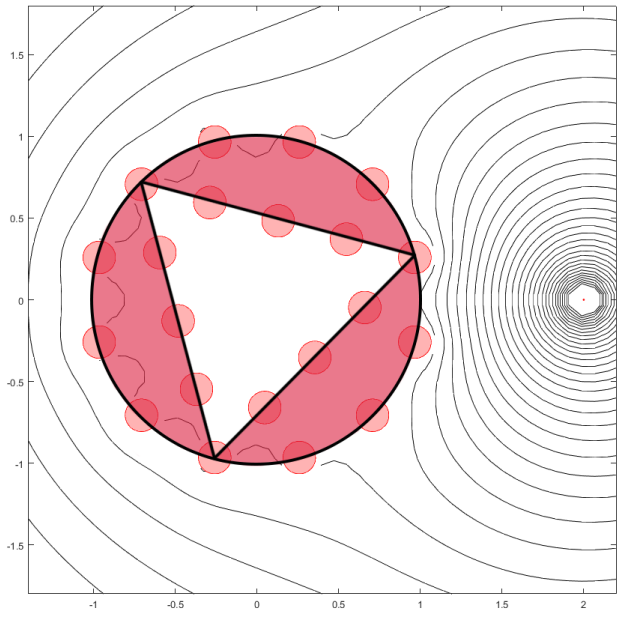

Figure 12: Surface area must be maintained when comparing cages of different shapes.

Looking at the image to our left, we can see that our method of constructing our polygons does not preserve the surface area within the cage, which could potentially be the cause of the results observed in table 2. In this image we have our standard cage and a triangular cage overlaid on top of each other. The red area denotes additional surface area contained by circle over the triangle, which in this case at least is significant. As the number of sides of our polygon increases it increasingly becomes similar to a circle, indeed we use a polygon with 360 sides and an approximation of a circle in our model.

To correct this we will maintain a fixed surface area of π for each of the polygons we examine. Alternately we could set the perimeter of our boundary as a fixed constant, this will form the basis of a specific problem tackled in section 5. Using this slightly altered methodology we can repeat our process and produce a new table of values comparing the polygons from our previous table.

Table 3: Varying number of disks and the shape of the boundary, whilst maintaining a fixed surface area.

	Triangle	Square	Circle
n = 5	0.0965	0.0947	0.1118
10	0.0160	0.0232	0.0236
20	0.0008	0.0006	0.0003
40	0	0	0

Maintaining a fixed surface area has affected our results however we still observe a somewhat unexpected pattern, a circular boundary does indeed produce the greatest protection for a boundary comprised of 20 disks but not for values of n less than 20. This behaviour will require additional analysis.

To gain a clearer understanding of the exact nature of the situation we reproduce table 3 including more values of n to attempt to identify the point at which the behaviour "flips". These new values are included below in table 4 and an associated plot can be found on the following page.

Table 4: Varying number of disks and the shape of the boundary, whilst maintaining a fixed surface area for 16 values of n.

	Triangle	Square	Circle
n = 1	0.5091	0.5084	0.5099
2	0.0465	0.1458	0.1463
3	0.1324	0.1561	0.1701
4	0.0349	0.1447	0.1438
5	0.0965	0.0947	0.1118
6	0.0637	0.0931	0.0839
7	0.0540	0.0613	0.0619
8	0.0276	0.0448	0.0453
9	0.0221	0.0321	0.0328
10	0.0160	0.0232	0.0236
11	0.0132	0.0167	0.0168
12	0.0093	0.0124	0.0119
13	0.0075	0.0089	0.0083
14	0.0053	0.0064	0.0056
15	0.0039	0.0045	0.0038
20	0.0008	0.0006	0.0003

By looking at table 4 to the left and figure 13 on the following page we can identify that the transition point at which a circular boundary becomes superior is at 15 disks. We note that by 20 disks the difference between the two configurations is very small, though if we consider this difference in light of the actual strength of the electromagnetic field this difference is quite significant.
As this is an unexpected outcome we may choose to analyse our testing methodology to try and identify any potential sources of error. One thought that springs to mind is that our results may simply indicate a triangular boundary provides the greatest shielding at the center point, but perhaps not if we alter our criteria for judging the "best" result.
Instead we may choose to use a slightly more rigorous criteria for judging the situation at hand. Previously we have solely been considering the strength of the electromagnetic field at a single point located at the center of the cage, however there are of course different means of comparison available to us.

We consider now possibilities in regards to establishing a suitable of comparing the different configurations of our cage. Ideally we would want to find some sort of average of the field strength within the cage, possibly also including the potential to check for "spikes" or the maximum value of the electromagnetic field within the confines of the cage. There are of course a number of different approaches that would be appropriate so we will now choose one suitable approach and proceed with our analysis, should our results prove suspect or lack sufficient detail we have the option of switching again to an alternate methodology.

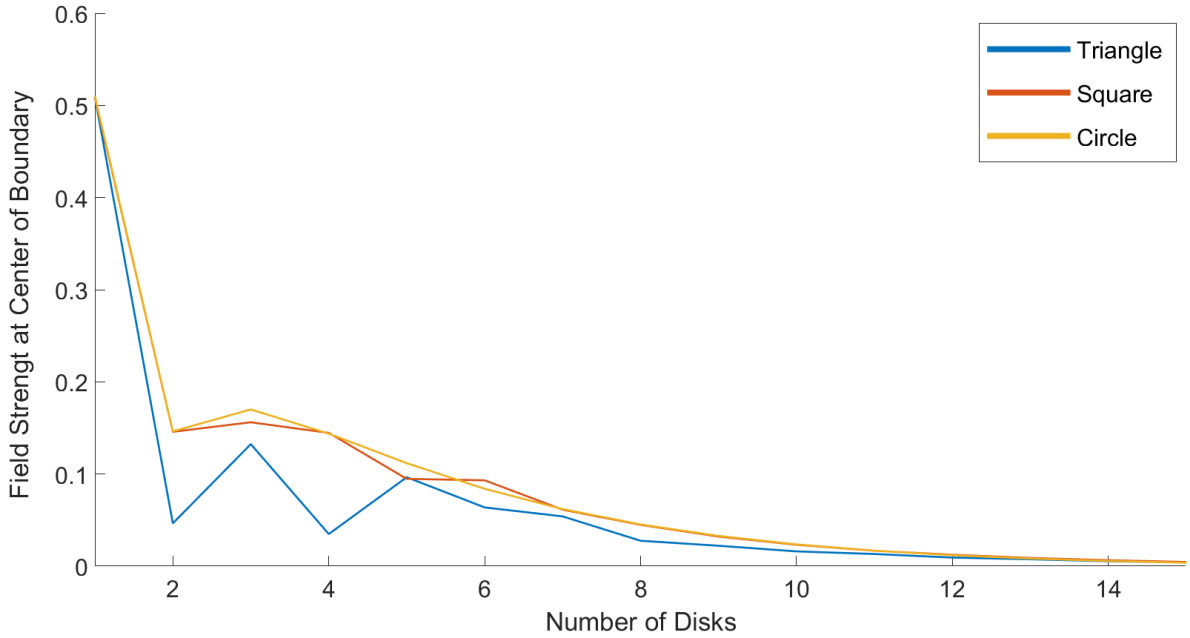

Figure 13: Plot displaying the effects of increasing the number of disks for several different boundary configurations using the value of the field strength at the center of the cage.

We adapt the following methodology. We treat the relevant area of the plane as a 1000 by 1000 grid comprised of one million individual points and then decide whether or not each of these points is within the boundary, if so the point is included in our calculations. We are then free to calculate various data based on these relevant points, for example the average field strength across these points or the maximum value of the field strength. The average field strength data obtained from this method is displayed in figure 14.

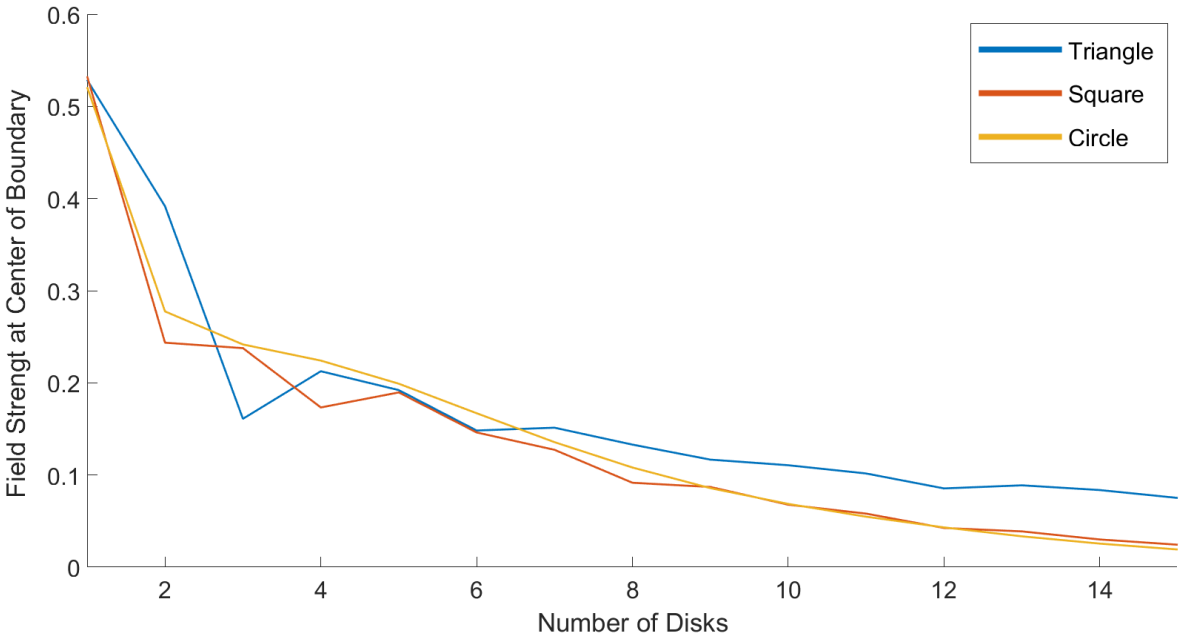

Figure 14: Plot displaying the effects of increasing the number of disks for several different boundary configurations using the average field strength within the cage.

This reveals a less clear-cut distinction between the different shapes at lower values of n, however we can conclude that a triangular boundary is in fact worse overall for values of n greater than 7. For values below 7 the ideal configuration depends on the exact number of disks used, this is most likely due to the boundary not being properly represented simply because the number of disks is too low. We can come to the conclusion that there is little difference between a polygon with 4 or more sides and a circle for values of n greater than 8, indeed if we were to add polygons with more sides we would see that they closely match the curves of the square and the circular boundaries seen in figure 14.

The complete set of data obtained from this alternate methodology may be seen in table 5 below.

Table 5: Varying number of disks whilst maintaining a fixed surface area, values calculated using alternate methodology.

	Triangle		Square		Circle	
	Average	Maximum	Average	Maximum	Average	Maximum
n = 1	0.5287	1.0690	0.5326	2.2307	0.5209	1.7336
2	0.3916	3.1993	0.2436	1.8921	0.2775	1.7302
3	0.1610	0.4716	0.2377	1.4978	0.2417	1.7329
4	0.2126	1.8647	0.1733	1.3285	0.2241	1.8358
5	0.1921	1.7702	0.1896	1.2924	0.1991	1.8160
6	0.1483	1.2238	0.1462	1.2844	0.1670	1.7392
7	0.1513	1.4226	0.1273	1.2346	0.1356	1.6352
8	0.1330	1.1507	0.0916	1.2003	0.1081	1.5191
9	0.1167	1.0143	0.0870	1.1049	0.0858	1.3987
10	0.1106	1.2002	0.0678	1.0324	0.0686	1.2786
11	0.1016	0.9906	0.0581	0.9580	0.0547	1.1612
12	0.0854	0.9278	0.0425	0.8598	0.0431	1.0476
13	0.0888	0.9072	0.0388	0.8370	0.0334	0.9387
14	0.0836	0.9129	0.0300	0.7481	0.0255	0.8346
15	0.0751	0.8478	0.0243	0.7605	0.0191	0.7354

We observe that the maximum value of the field strength within the boundary is lowest for a number of values of n below 14 for the triangular boundary for values of n below 14, at which point the circle is superior. This supports the idea we have formed that for a low number of disks the behaviour of the cage varies highly based on the particular value of n rather than fitting an easily observable pattern. It is worth noting that the results we have obtained have been for a radius of 0.1mm which is the largest value we will be considering, if we wish to obtain significant shielding for wires of radius say 0.001mm, we will need to use a large number of disks and as such we can use a circular boundary, assuming it to be optimal.

To make one final observation, based on the behaviour of figure 14 we can say that it is likely that polygons with more than three sides have an average field strength that converges to zero in a similar manner to each other. Whilst this seems to be the case we lack a proper sample of polygons to be able to make this statement with confidence, our current results only containing three values of n which is only enough to give an indication of a possible trend. To confirm this idea we plot this set of results once more, this time with a larger selection of regular polygons with increasingly many sides. Should our expectations prove correct we would expect the results to trend towards those of the circle as the number of sides increases. The resulting plot, figure 15, may be found on the following page.

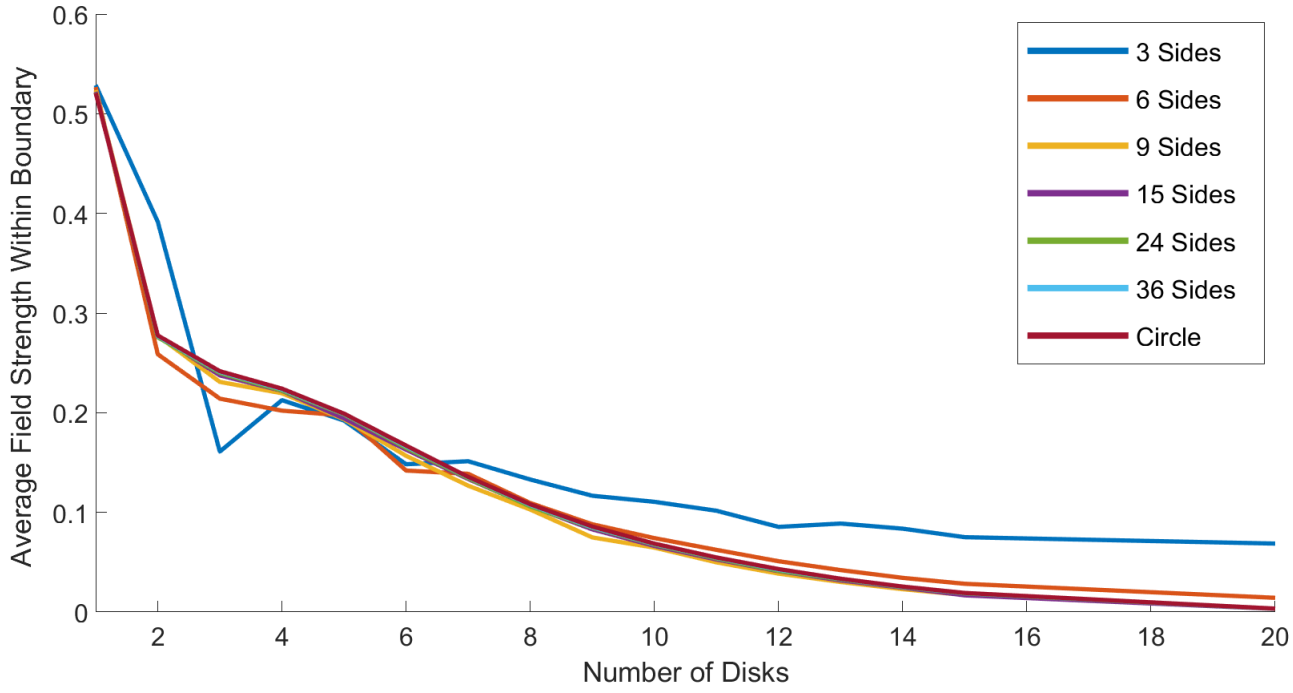

Figure 15: Plot displaying the effects of increasing the number of disks for a large number of different boundary configurations.

This confirms our conjecture, meaning henceforth we can assume that as the number of sides of our polygon shaped boundary increases it increasingly conforms to the behaviour of a circular boundary, with circular boundary providing the optimal amount of shielding. We can also say that this occurs very quickly, requiring only a 4 sided polygon to achieve near matching results to those of the circle.

Now that we have analysed the initial situation we may move on to more complicated scenarios, the first of which will be considering the effects of using multiple Faraday cages in unison.

4 Multiple Faraday Cages

4.1 Analysing the Situation of Multiple Cages

Our general aim is to maximise the shielding provided by the Faraday cage therefore minimising the strength of the electromagnetic field within the confines of the cage, so initially we will analyse the general situation of multiple Faraday cages interacting and then gradually move towards a definitive conclusion based on our model. Starting from a less specific situation will allow us to have a greater degree of confidence in our results making it the ideal way to proceed at this point in our analysis.

To begin let us attempt to determine the general effects of adding a second cage. To do this we introduce a second cage into our model, contained within the first. For the first cage we maintain a fixed surface area of π and for the second a fixed surface area of $\frac{\pi}{4}$, and we choose to have both of these cages possess the same shape, e.g. both circular. Maintaining a fixed surface for both cages will allow us to avoid the problems that arose in section 3 regarding different cage configurations providing shielding for areas of different size. Furthermore to obtain clear results we choose to use a radius of 0.01mm rather than 0.1mm for our wires, as otherwise the values obtained would be very small and as a result there would be greater for error. We note now that will be using our alternate methodology for calculating the average field strength within the cage as we will be using a triangular inner cage for some of our results and as such will need to ensure that our means of comparison is reflective of the situation.

Shown to the right in figure 15 is the general situation at hand. For now we will focus on results for the simpler cases, where both the inner and outer cage are of the same shape. Once we have done this we will then incorporate more complicated situations into our results after having first established a general sense of what we might expect. It is quite possible that a particular combination of cages may prove optimal, rather than simply using two circular cages as one might first expect, however the existence and exact nature of this combination will only become clear after having scrutinised the relevant data.

Shown below in figure 16 is a plot showing the data obtained for the simpler cases as mentioned, on the following page figure 17 displays the data obtained including all possible combinations of cages where the possible cage shapes are triangular, square, and circular.

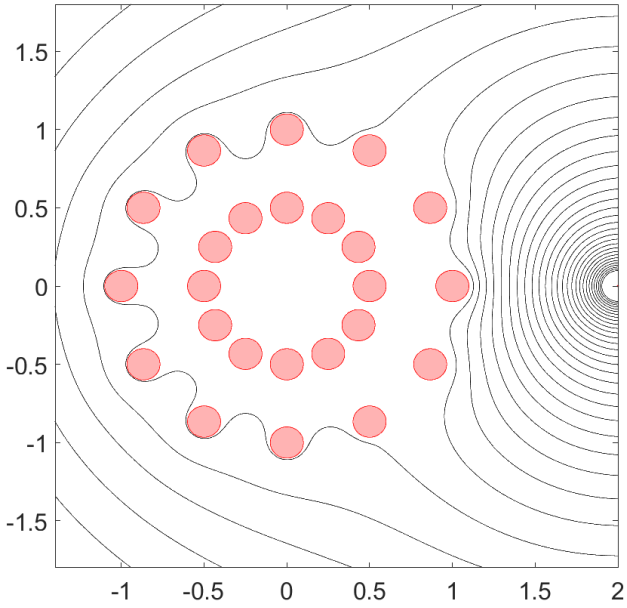

Figure 16: Two Faraday cages used in conjunction with one another with both inner and the outer cages being circular.

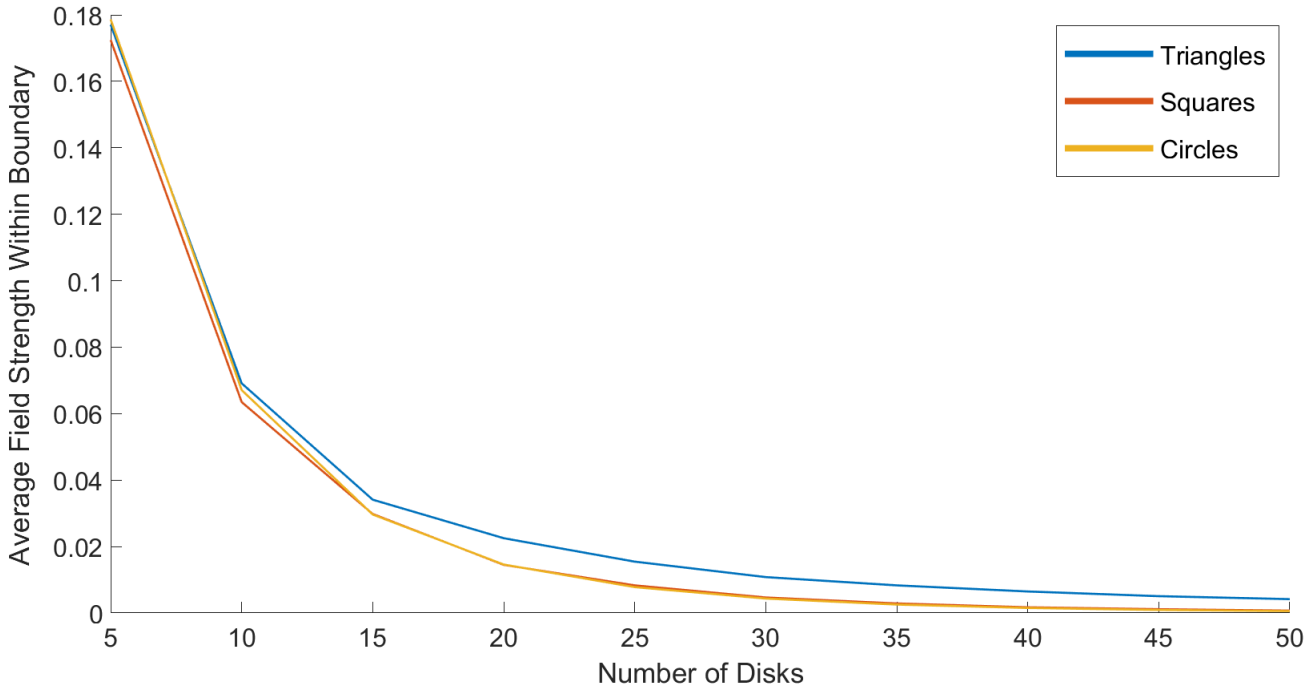

Figure 17: Plot displaying the effects of increasing the number of disks for two Faraday cages used in conjunction with one another, both of which possessing the same shape.

We can observe that the data is in line with what one might expect, based on the case of the initial test problem. We have that the optimum configuration consists of two circular boundaries, with the "worst" configuration consists of two triangular boundaries.

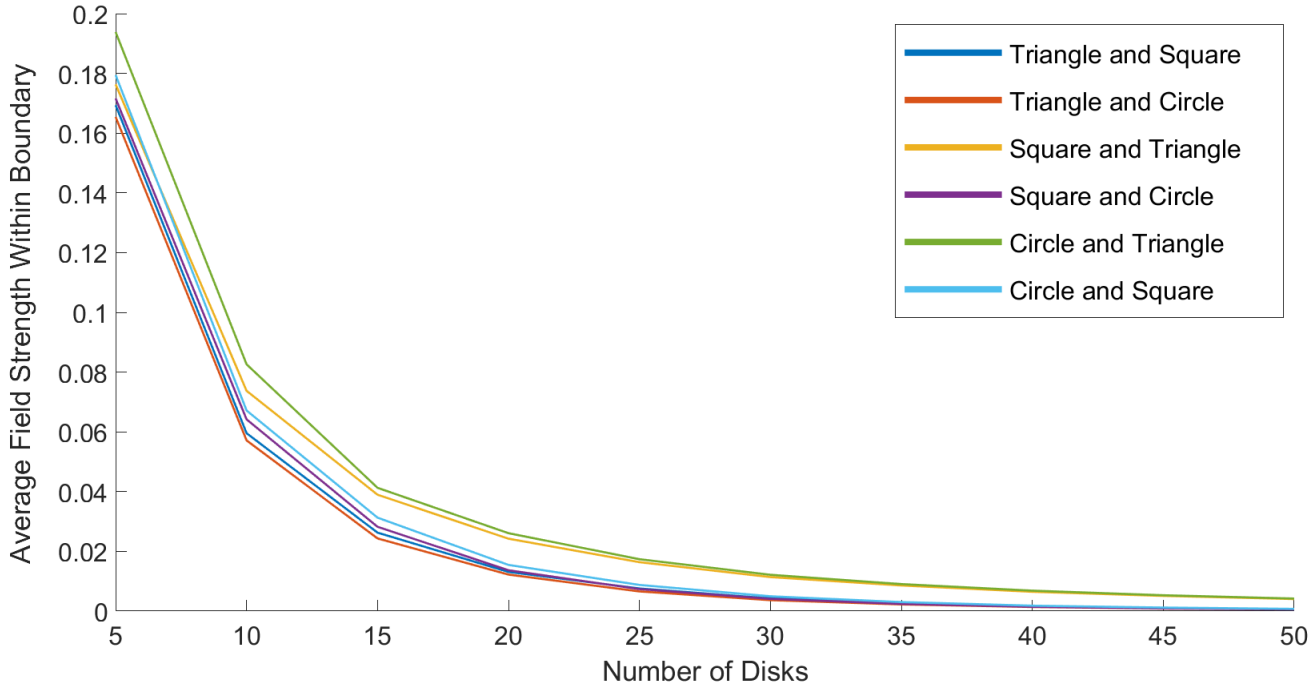

Figure 18: Plot displaying our six possible configurations, the first shape listed is the shape of the outer boundary whilst the second is the shape of the inner.

Looking at the obtained data we are able to draw some conclusions. The "best" configuration includes a triangular outer boundary, whilst the "worst" includes a triangular inner boundary. This lines up with previous results despite appearing unusual at first glance. We have previously found that a triangular cage is effective at minimising the field strength at the center, but proves inefficient when all points within the cage are averaged. This naturally is a beneficial property for multiple cages as the inner cage contains those points located around the center of the outer triangular boundary. It would seem that the negative nature of a triangular inner cage is dominant in this situation, even if composed with a triangular outer cage.

It appears that if we avoid a worst case scenario the difference between cage shapes is minimal for a polygon with four or more sides and any other such polygon. Therefore if we use multiple Faraday cages we should choose a triangular outer cage and a circular inner cage, with choice of the inner cage being of lesser importance so long as it is not triangular. This claim is true for most standard cases however if we have a situation in which we solely wish to maximise shielding at the center then it would be better to use a composition of two triangular cages. This would also be the case if this area around the center is increased slightly, with the point at which the optimal switches being dependant upon several different factors.

4.2 Optimal Use of Material

Having investigated the effects of using two Faraday cages in unison we may now move onto a more complicated question. If we have a limited amount of material from which to form our disks, what is the best configuration available to us?

When answering this question we will need to make use of the knowledge of the general situation we have built in previous sections, considering how to provide optimal shielding for the case of one shield and for two cages. We will only consider these two possibilities as these are two situations we already have experience with and utilising more cages would massively increase the complexity of the situation.

To tackle this problem we simply extend our earlier tactics appropriately. We set a fixed surface area to be shielded as effectively as possible and a fixed number of disks to be used. We then compare the results of one triangular cage against those of our optimal configuration for increasing values of n. We choose a triangular cage based on previous results showing it to be optimal for minimising values at and close to the center, the region of the inner cage. Results are provided for the average field strength within the confines of the inner cage.

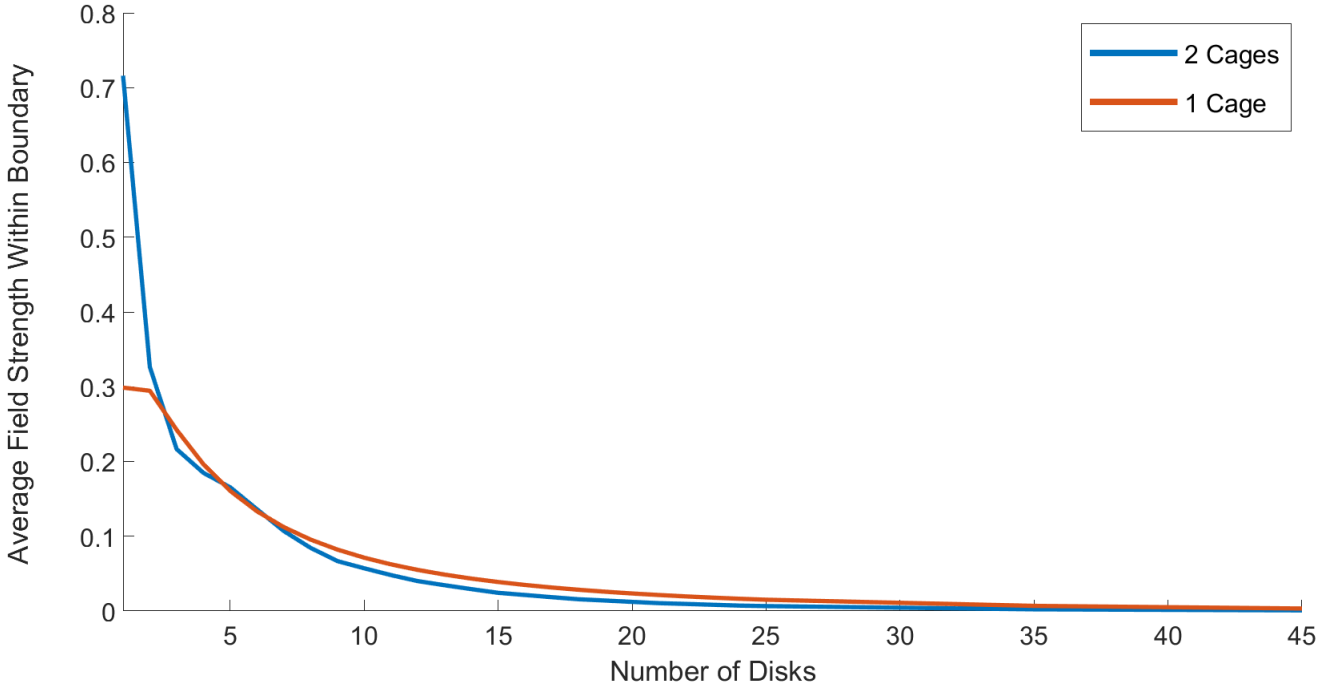

Figure 19: Plot displaying the average field strength within the region of the inner cage for one cage and two cages, with a fixed wire radius of 0.01mm.

From this data we can conclude that using two cages is optimal, or very close to it, for all situations except for the trivial case. The difference between using one and two cages is not massively significant but using two cages is slightly more effective at shielding the region within the inner cage for a value of n between 7 and 30, before and after which the difference is negligible.

5 Specific Problems

5.1 Microwave Application

In this section we will tackle several, more specific problems related to Faraday cages through utilising our model. Previously we have analysed some general situations that arise when dealing with our model, now we deal with one final one with the intention of providing some insight into a more specific problem. This is attempting to understand the effects of varying the source location on the shielding provided by our cage. In particular, what happens when our source is located at the center of our cage?
Using a similar approach to one used in section 3.1, we can obtain a set of results by varying the radius of the wire and the number of disks composing the cage. These results are obtained using a circular cage, as we have previously deemed it to be at the very least, near optimal for sufficiently many disks.

Table 6: Varying radius of the wires composing the disks and number of disks for a circular Faraday cage with electromagnetic source located at its center.

	r = 1	0.9	0.8	0.7	0.6	0.5	0.4	0.3	0.2	0.1
n = 5	1.8241	1.0785	1.2790	1.5062	1.7419	1.9616	2.1567	2.3175	2.4375	2.5132
10	0.8447	0.9195	1.2015	1.3604	1.6229	1.8465	2.0444	2.2231	2.3841	2.5024
20	0.7113	0.8067	1.1321	1.3407	1.6041	1.8066	1.9920	2.1382	2.3221	2.4701
40	0.5639	0.6046	1.0643	1.3264	1.5611	1.7799	1.9450	2.1564	2.2992	2.4418
80	0.4612	0.7905	1.0614	1.3319	1.5619	1.8094	1.9464	2.1299	2.2912	2.4320
160	0.4386	0.7906	1.0769	1.3312	1.5632	1.7597	1.9009	2.1364	2.2829	2.4285
320	0.4263	0.7890	1.1275	1.3372	1.5631	1.7998	1.9585	2.1305	2.2853	2.4193

It is immediately apparent that the results obtained show we need to use a combination of a large number of disks composed with very thick wires in order to cause a significant decrease in the electromagnetic field strength outside of the cage. We note that it appears as though placing the source inside of the cage makes it significantly harder to minimise the average electric field strength in the remaining region. To see significant reduction in the field strength we require disks comprised of wires of very thick radius and we require a large number of these disks.

Now we have developed an idea of the results we should expect we may move onto applying this knowledge directly to a problem with potential real-life application. A common application of the Faraday cage is in the microwave, a device found in almost every home that uses electromagnetic waves to cook food. The body of the microwave comprises a typical Faraday shield with the exception of the door, which rather than being comprised of a metal sheet is instead a metal mesh placed between two sheets of glass. This is to allow the inside of the microwave to be seen whilst the food is cooking, whilst at the same time blocking the harmful microwaves from being emitted into the surrounding area.

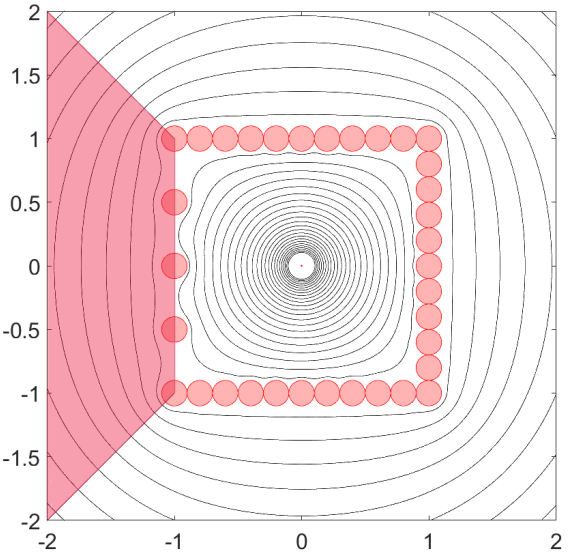

Figure 20: Our new configuration. The section highlighted in red is the area over which we will be measuring the average strength of the field.

Using our previously established framework we can model this situation and experiment with modifying the conditions to try and come to some conclusions about the nature of the situation. It is immediately apparent that we need to modify our situation slightly from those we have seen before. There are three key points that we need to address in order to successfully reconfigure our model.

Firstly, we need to move the location of the electromagnetic source, previously we positioned the source outside of the cage, however now we wish to place the source inside and attempt to minimise the strength of the field exterior to the cage. Based on the results obtained at the start of this section we can assume that we will need to use a large number of disks, each with a large radius, in order to achieve significant shielding. We also have a good idea of the general range of results we should expect after running our model.

Secondly we need to change our boundary, rather than using a boundary that is uniform on each of its sides we wish to mimic the appearance of a microwave. Using a two-dimensional approximation we arrive at the figure 19, three sides are effectively solid, approximating the walls of the microwave, whilst one is comprised of fewer disks, the "door".

Finally we need to adjust our judgement criteria, using the field strength at the center of the cage is no longer possible so we must use an adaptation of our alternate methodology. Now we choose to find the average of the field strength for each point in the area outside of the door, this is the red area shown in figure 20 on the previous page.

Below figure 21 shows results obtained using this approach.

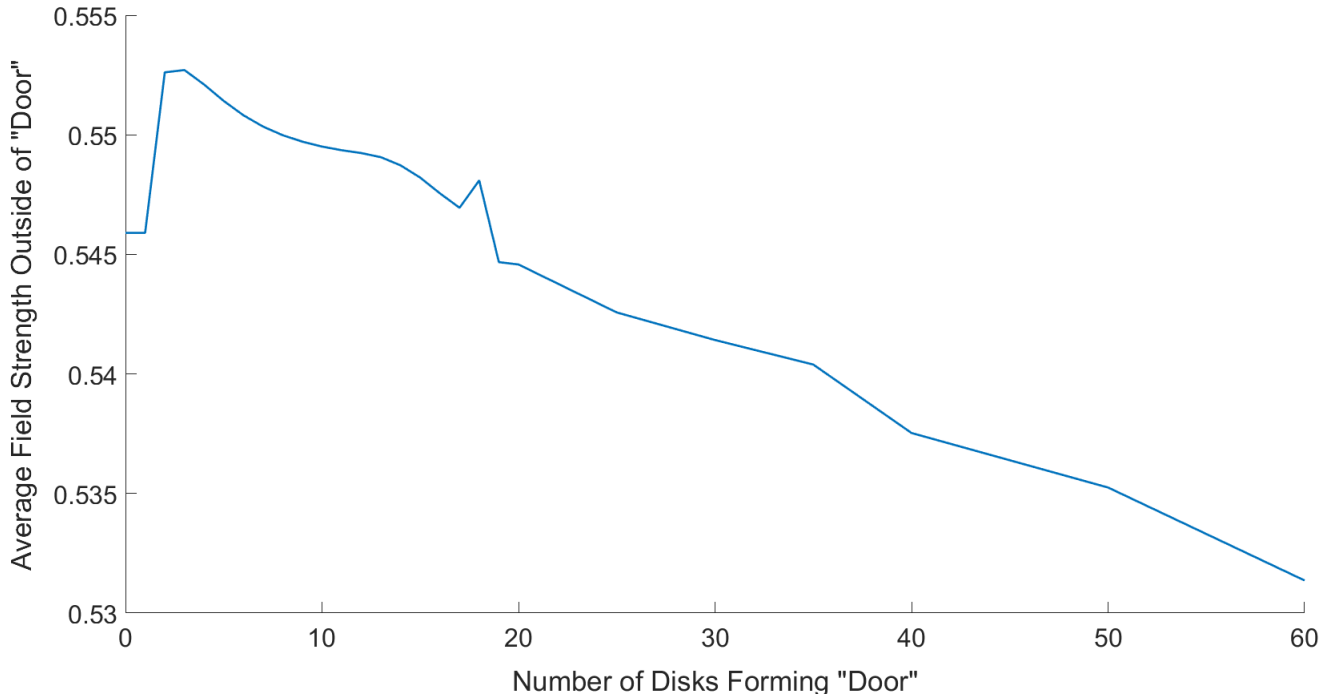

Figure 21: Plot the effects of increasing the number of disks forming the "door" in our two dimensional microwave model with "walls" comprised of 10 disks each.

We can observe that between 2 and 18 disks the average field strength outside of the door is higher than if we were to use only 1 disk, which is somewhat surprising. For more than 19 disks the field strength gradually decreases, as we would expect it to.

We also note that the difference in the field strength is relatively minor, differing by only around 0.2 at most. This leads us to the conclusion that the number of disks comprising the door is relatively unimportant, except in the case of a large number of disks. This matches with the reality of the situation in which a metal mesh is suitable for blocking the electromagnetic radiation to a sufficient extent.

Having considered this approximation of a microwave we now move onto another specific problem that is grounded in reality. This problem is how best to maximise shielding for a given area when only a limited quantity of material is available to be used. This problem is quite similar to one tackled previously, however specifying a given area will lead to changes in our examination of the situation. We will move into dealing with specific quantities which will complicate the problem further whilst providing more comprehensive answers.

5.2 Maximising Shielding for a Given Shape

Initially we will simply test a number of different regions and find the optimal shape of the cage to best protect them. The answer to the question will most likely heavily depend on the size of the area we wish to protect, as we have seen previously a triangular cage is effective at protecting the region near its center but provides poor shielding at its extremities.

An example of one particular situation may be seen to the right, here we wish to minimise the average field strength within the blue square. Due to the method we use here it is relatively simple to use a variety of different shapes and look for common trends. This approach involving using a similar tactic to our methodology for finding the average field strength whilst only including those points that are contained with the area of interest to us. Exact details of this approach are provides in Appendix B.

Results obtained for the square region shown in figure 22 are shown in the plot below.

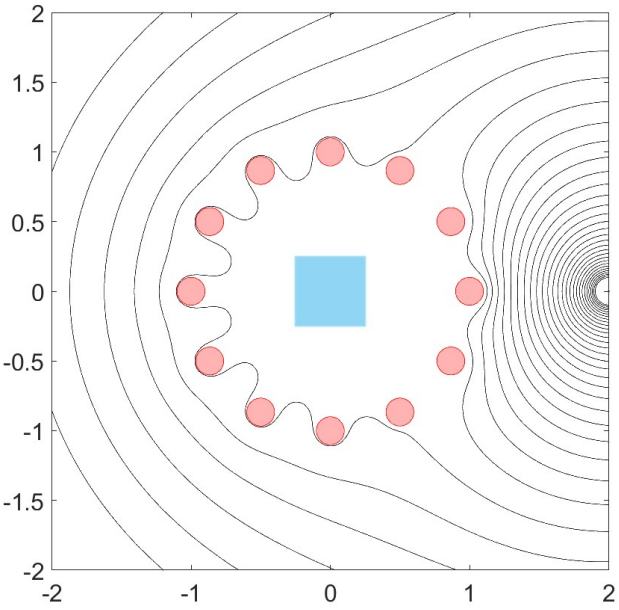

Figure 22: Our usual model consisting of a circular Faraday cage with the addition of blue square highlighting the area over which we will be finding the average field strength.

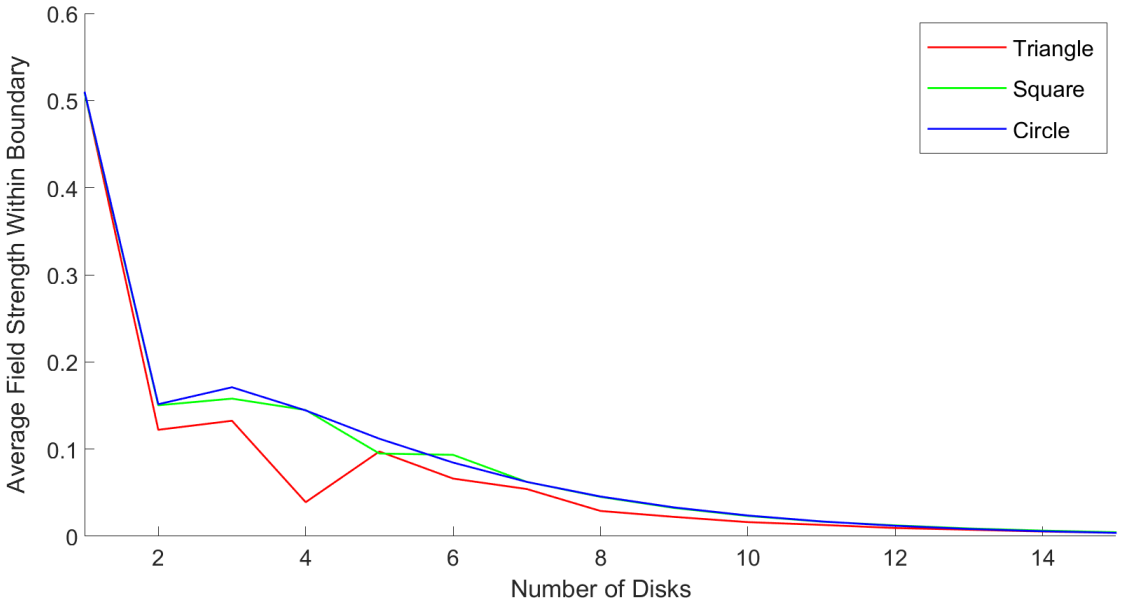

Figure 23: Plot displaying the effects of different shaped boundaries on the average field strength as the number of disks increases, within the confines of the protected region.

These results match those obtained earlier, as expected a triangular Faraday cage is most effective at protecting the area closest to the center. It would be expected that the optimal shaped cage to use would depend on the size of the shape, as well as the proportion of its surface area that is located near the center and the number of disks that are used to form the cage. For smaller regions located near the center of the cage this will generally be a triangular cage, otherwise a circular cage is optimal. Results were also obtained for the protection of a triangular and a rectangular region, with the obtained plots bearing extreme similarities to figure 23.

Should we wish to maximise shielding for the region using a limited quantity of material with which to compose our disks, the problem becomes more complicated. In this case it is generally best to use two Faraday cages, as we have shown in section 4 that this provides optimal shielding for any number of disks above 1. We have previously found that a circular inner cage composed with a triangular outer cage provides optimal shielding for the region comprised of the inner cage, meaning the optimal cage composition will likely either be this, or two triangular cages if the region we wish to protect is small and close to the center.

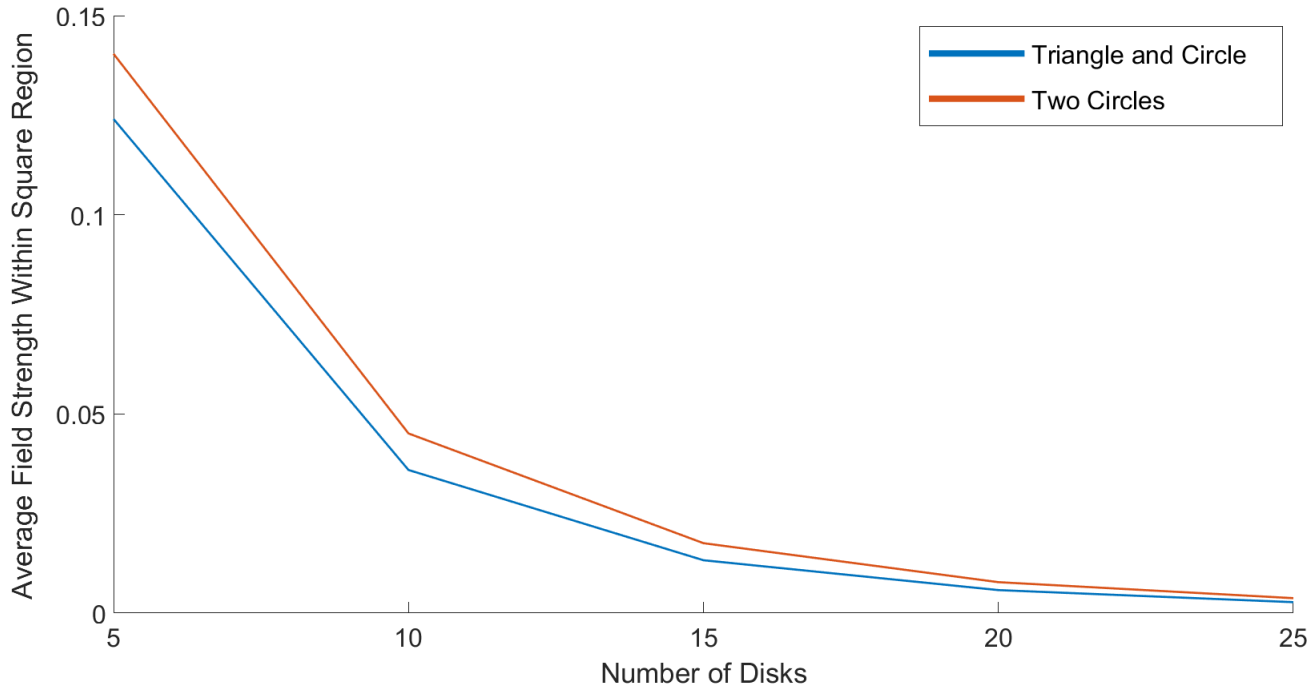

Figure 24: Plot displaying the effects of different shaped boundaries on the average field strength as the number of disks increases, within the confines of the protected region.

As finding an optimal configuration depends on the region we wish to protect we will cover a test region and proceed through the general process of finding an optimal arrangement. We will arbitrarily choose to maximise shielding for a square region as the method is functional regardless of the shape chosen. To determine the ideal choice of cage shapes in the case of two cages we simply calculate the average field strength within the square region for each of our two possible configurations, for various numbers of disks. The results obtained are shown above in figure 24. We can clearly see that the configuration consisting of a triangular outer cage and a circular inner cage is optimal for all values of n and so we choose to use this configuration for this region. This will maximise the average shielding for this region, allowing us proceed to accounting for quantity of available material.

As we are interested in maximising shielding in our region for a fixed quantity of material we will now need to determine the ideal radius of disk to use, as well as the number of disks we can form using the amount of material we have. Testing for various values shows us that it is generally better to use disks with smaller radii, which can be seen quite clearly by creating a test situation and making use of our model.

Suppose we have $1mm^2$ of material available to use to form our disks, assuming that we use this material to form only complete disks this means that if we use disks of radius 0.5mm then we can form 1 disk, alternately we could use disks of radius 0.3mm and form 3 disks, or 0.2mm to form 7, and so on.

Table 7: Table displaying the effects of using disks of different radius on the field strength within the boundary for a circular inner cage and triangular outer cage. When the number of disks is odd the extra disk is assigned to the inner cage.

	Number of Disks	Field Strength at Center	Average Field Strength
r = 0.5	1	0.6452	0.6463
0.4	1	0.6239	0.6249
0.3	3	0.1581	0.2332
0.2	7	0.0059	0.0148
0.1	31	6.3200*10^(-7)	1.7022*10^(-6)
0.05	127	1.2126*10^(-9)	1.7263*10^(-9)
0.01	3183	6.4243*10^(-8)	6.5582*10^(-8)

These results indicate that the optimal radius of disk to use is somewhere in the region of 0.1mm to 0.01mm, with further testing revealing that the optimal radius is exactly 0.05mm , correct to 2 decimal places. Using this disk radius will provide us with an optimal configuration.

If we were to wish to find the optimal configuration for some other amount of material, or perhaps for a different area, then the process for finding the optimal cage configuration would be much the same. That would be following the approach outlined above with the possibility of some decision points being different, this remains simple as the "correct" choice at each point is purely based of the output obtained from our model.

5.3 Possible Improvement to Disk Placement

The final specific problem we will be covering concerns a re-evaluation of the optimal means of arranging our disks. Previously we have chosen a polygon and spaced our disks equally along the boundary, this would naturally mean each disk is an equal distance away from the two disks adjacent to it. There are however alternate ways we can arrange our disks whilst still keeping the total number of disks the same. For example we have considered the possibility of using two Faraday cages, one contained within the other, and splitting the number of disks available between these two cages. Now we consider the possibility of placing our disks not at equally spaced intervals, but rather at points corresponding to angles. This will lead to only a minor difference in the placement of the disks however this small adjustment could very well lead to an improvement in the effectiveness of our cage configuration and as such is worth exploring.

Visual clarification is provided in figures 25 and 26 at the top of the following page. The difference shown in figure 26 between our previous approach and our new one is subtle, the gap between the center of the disks and the intersection of the lines with the polygon being quite small and difficult to observe at first glance. It is worth noting that as we increase the number of disks this small displacement becomes increasingly relevant as with each disk added the difference between our two configurations grows larger.

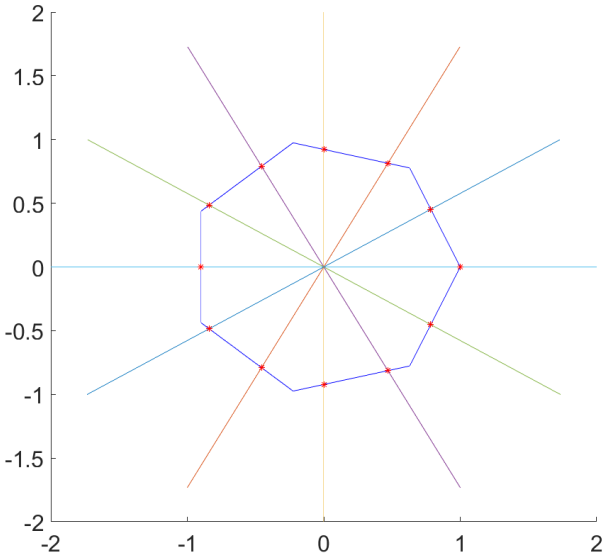

Figure 25: A configuration of disk locations based on our new methodology, using a polygon with seven sides and a separation of 30° between neighbouring disks.

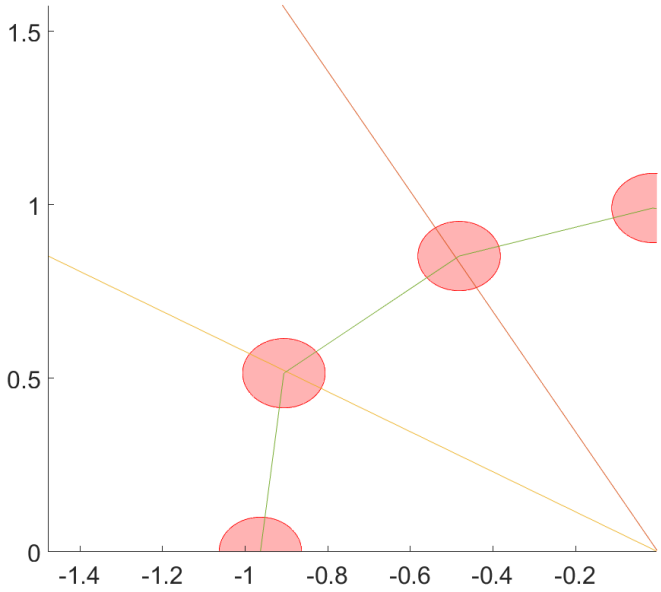

Figure 26: The various lines passing through the origin correspond to 30° intervals, whilst the disks correspond to the location of the disks the approach of equal distances between disks.

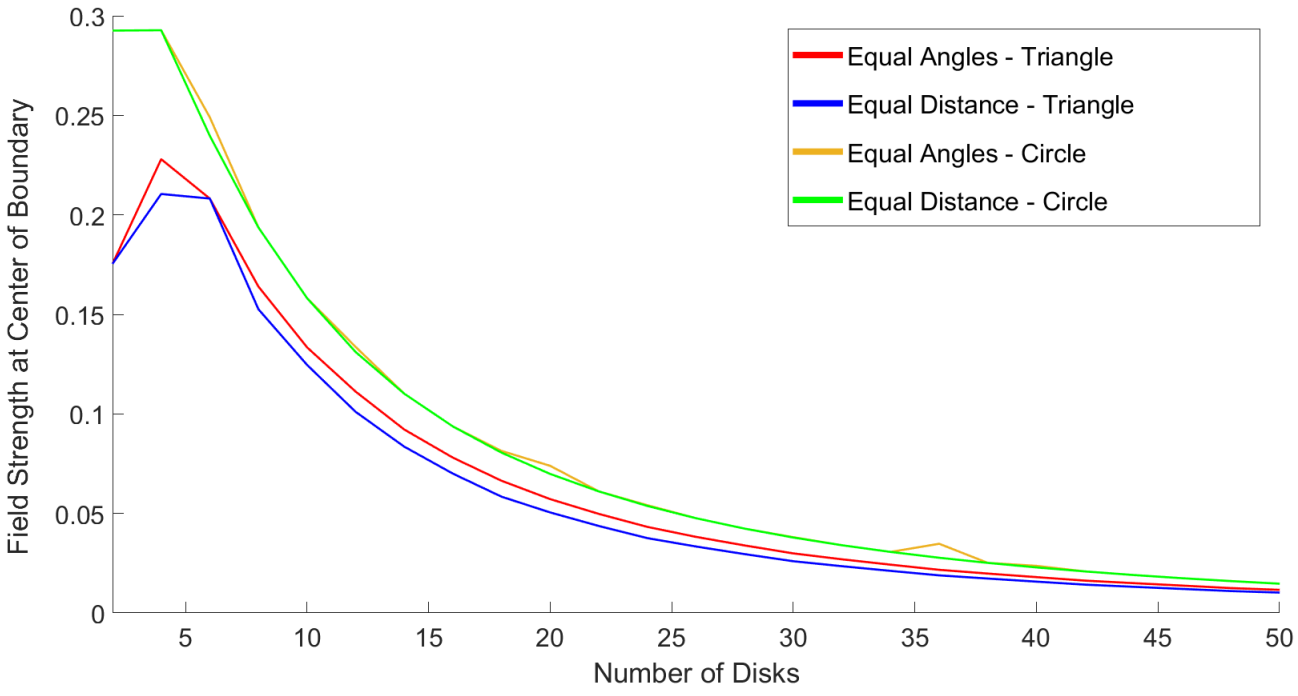

Figure 27: Plot displaying the effects of increasing the number of disks on the field strength at the center of the boundary with a fixed disk radius of 0.01mm for both a triangular and circular boundary and for both approaches.

To compare the two approaches we calculate the field strength at the center of the boundary for each of the two approaches whilst varying the number of disks available. The results obtained are displayed on the previous page in figure 27.

As expected the results produced by each of the two approaches are quite similar to each other, however we do notice some interesting differences. It appears as though this alternate approach proves to superior for the case of a triangular boundary, though it provides virtually identical results for a boundary in the shape of a regular polygon with more than 3 sides. Figure 27 shows the similarity of the results found for the two approaches for a circular boundary, while further testing showed very similar results for a selection of polygons with more than 3 sides.

These results suggest that if we are interested in utilising a triangular boundary then it would best to use this alternate methodology when deciding the placement of the disks rather than our previous approach.

The results of this particular test indicate that there may still be some room for improvement in regards to our previous results, although only in results that involve a triangular boundary in some respect and in these cases the amendment is quite easy to make. To amend these results we would simply need to use the code for this approach (provided in Appendix B) rather than the general formulation (provided in Appendix A).

Having finished tackling these specific problems we now move onto discussion of possibilities concerning extending our general model.

6 Further Extensions of Results and Potential Applications

6.1 Extension to Three-Dimensions

The results obtained throughout the course of this dissertation have been collected using a two dimensional model approximating the behaviour of electromagnetic waves interacting with Faraday cages. These results provide an idea as to the general behaviour of the situation, however they are lacking when it comes to approximating reality in a complete sense as they do not extend to three dimensions. In order to extend our model to three dimensions we would need to deal with the problem of increasing the number of calculations that need to be made by MATLAB, for some of the plots produced the calculation time has already increased significantly from only a few minutes to around an hour or so. Care would need to be taken in order to prevent this from becoming a problem when using the model as one of the major strengths of the current approach is the ability to obtain near immediate results. This allows for experimentation and for adjusts to be made as needed.

In terms of constructing a suitable model one possible solution may be seen in reference [6]. In this case the author uses a theoretical approach via Green's function, which could be considered a natural extension of the two dimensional model used here. To extend his results to three dimensions the author treats the problem as two dimensional by treating the z-direction as infinite and solving the two dimensional case, confirming his results through practical testing.

An alternate possibility would possibly be iterating the two dimensional model a number of times, using different configurations to approximate the situation at different points on the z-axis. Essentially using a number of two-dimensional models to build up an idea of the three dimensional case. This would definitely massively increase the computational time needed to produce a solution, however this may be able to be reduced to an acceptable level through streamlining the required code. The initial model is a result of Trefethen's work on ten digit algorithms and as such is very efficient, making this approach potentially feasible.

It is likely that in three dimensions the nature of the model would bear some similarity to the results obtained here for the two dimensional case. For example in section 3 we obtained results showing that the average electric field strength within the boundary decreases as the number of the disks forming the cage increases, this would likely be the same in three dimensions though the exact nature of the relationship may differ.

6.2 Alternate Extension Approaches

If we expand our focus away from being purely concerned with this particular model for characterising the situation there also exist some interesting possibilities for better understanding the mathematical behaviour of a Faraday cage. In [1] three models are presented to analyse the situation, while over the course of this dissertation we have dealt with the first of these models however the remaining two models are of course also worthy of discussion. One of these models uses an observation that inside of the a circular cage the change in the potential at different points can be approximated with a smooth function to produce a continuum approximation.

This approximation is used as a tool in [9], the authors D. Hewett and I. Hewett were able to extend the initial analysis of [1] in a number of ways: generalising to arbitrary wire shapes (not necessarily circular disks), investigating the case of "thick" wires, and analysing the analogous Neumann problem, where there are small gaps between wires.

An example of the work done in [9] can be seen in figure 27. Here rather than forming wire into disks which we then use to form our Faraday cage instead we simply require that the wires be formed into non-intersecting, compact subsets of the plane all with the same shape. This leads to some interesting conclusions regarding how the electric field strength within the cage is affected by the particular shape of these individual disks. It should be noted that the results obtained are purely for the case of a circular boundary, as was the case for the results found in the original article that formed the basis of this dissertation, reference [1].
It would potentially be feasible to implement this alternate formulation in MATLAB and apply the code used in this dissertation to it, however this would require first formulating the alternate model based around a continuum approximation. This is outside the scope of this dissertation but would certainly be a topic worthy of investigation.

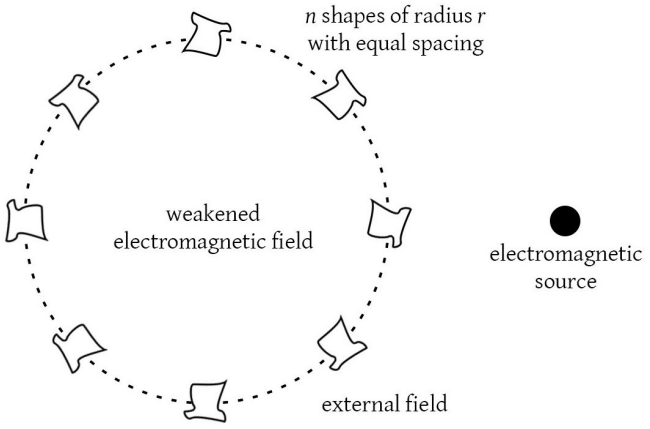

Figure 28: Our usual configuration with our usual circular disks replaced by an alternate shape. This alternate shape is rotated to preserve its orientation towards the center of the boundary at each point it is placed on the boundary.

At this point we move from possible extensions to relevant models to considering the potential applications these models may have in various fields.

6.3 Potential Applications

A practical application for a Faraday cage can be found in reference [10], in which the authors attempt to minimize the strength of the electric field below an active power line through the use of various different materials. This is a simple scenario and as such is a good starting point as we move on to considering real life situations.

In this article the authors use a purely practical approach, conducting tests using several different materials and recording the results obtained. This is a functional strategy for a small-scale investigation however if we were to increase the number of materials available and introduce other possible factors then we would quickly find ourselves struggling to conduct the physical testing needed to arrive at a solution. However if we were to use a suitable model in conjunction with practical testing we would likely be able to reduce the number of possible obtains down drastically. The basic situation present in this paper may be seen in figure 28.

A somewhat more complicated example can be found in reference [5] where a copper-foam based Faraday cage is used to provide shielding from an ion bombardment and affect the growth of graphene. As with the previous example it would perhaps be sensible to make use of a model such as the one that is the focus of this dissertation in order to produce the desired outcome. Naturally a more complicated problem will often necessitate a more sophisticated model, however the core principals remain the same.

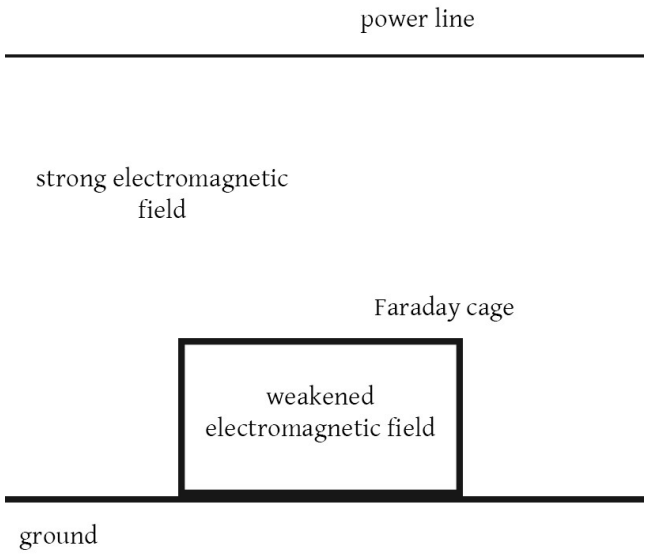

Figure 29: The scenario presented in reference [10]. Here we have a Faraday cage placed below an active power line with the goal being to minimise the strength of the electric field within the cage through the use of different materials. The strength of the electric field is measured using a sensor placed within the cage.

There of course other applications for Faraday cages, for example article [5] is but one instance of a common application, that being in the field of biology. Faraday cages are often used in conjunction with biosensors and immunosensors in a wide number of different pursuits. As mentioned reference[5] mentions the use of a Faraday cage to provide shielding from an ion bombardment to affect the growth of graphene, while in reference [**?**] a Faraday cage is used to overcome low electrode reaction efficiency by providing shielding for the reaction. The exact nature of the application differs massively across the field but in many of these cases is an invaluable tool albeit one that requires careful utilisation in order to manifest the desired effect. As previously mentioned this is where the use of a model is particularly important, the ability to accurately predict the exact effects of the cage is essential.

Having briefly covered potential areas in which this particular model may be extended and how general situations involving Faraday cages may be further analysed we now move onto a summation of the results obtained over the course of this dissertation.

7 Conclusion

Throughout the course of this dissertation I have attempted to provide additional clarification to the details of the model put forward by Chapman, Hewett, and Trefethen in their article "Mathematics of the Faraday Cage" [1], as well as extend the general results obtained from this model and apply it to some specific situations of interest. In this final section I will summarise the results obtained, leaving the two appendices to explain the MATLAB code used to obtain these results in detail.

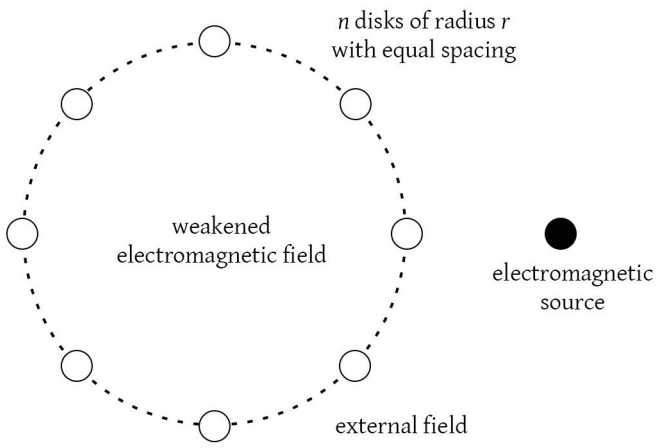

Figure 30: A Faraday cage comprised of 8 disks placed on the boundary of a circle.

The situation we deal with is generally quite simple, we form a Faraday cage comprised of a number of disks placed along a boundary layer and then seek to minimise the strength of the electromagnetic field within the boundary. This can be done by either seeking to minimise the field strength at the center, or on average inside the boundary. In most cases the shape of this boundary layer will be that of a regular polygon, often a circle.
This situation is suitably modified when dealing with particular scenarios, however these modifications only affect parts of the situation or add to it rather than being substantially different. This means we can simply amend this general situation and alter our model as needed without major difficulty.

Through using a standard configuration of a circular boundary and measuring the field strength at the center we obtained results for the simplest situation, altering the radius of the wires used to form the disks as well as the number of disks used. This showed us that increasing either radius or number of disks resulted in a decrease in the electromagnetic field strength at the center of the boundary, with it appearing that the number of disks was the more important factor.

We then tested the effects of changing the shape of the boundary layer, realising that we needed to maintain a fixed surface area if we wanted to obtain meaningful results. We concluded that a circular boundary is optimal once the number of disks has passed 11. We repeated our tests using an alternate methodology, testing the average field strength within the boundary rather than the field strength at the center, which coincided with our earlier results and lent further weight to the idea that a circular boundary is optimal. After a final point regarding the nature of the n-sided polygon forming the boundary and its effects on the field strength within, we moved onto dealing with the situation of multiple Faraday cages working in tandem.

By starting with a simple situation we managed to conclude that if using two Faraday cages of the same shape it is best to use two circles, though the distinction between circles and any n-sided polygon where n is greater than 3 is minimal. Building upon this idea we analysed the situation of any two Faraday cages working together, which proved to have a more complicated solution, relating back to the behaviour of an individual cage of varying shape.

If we seek to minimise the strength of the field at the center, then a triangular cage is better for low numbers of disks as a triangular cage provides effective shielding near center points but comparatively weak shielding at points near its extremities. For this reason it is best to use a circular inner cage, to maximise the average shielding within the inner boundary, and a triangular outer cage, to maximise the average shielding in the area around the center point.

When we compare a singular Faraday cage against the composition of two Faraday cages, whilst maintaining a fixed amount of material with which to protect our inner region, we see that generally the two situations are equivalent, with two cages being slightly superior for lower number of disks.

At this point we moved onto tackling more specific problems the first of which was the real-life application of a Faraday cage to a microwave. After some initial tests to better understand how moving the electromagnetic source inside of cage effects the results obtained we brought a two-dimensional simplification of the problem into our MATLAB model, this allowed us to experiment with changing the number of the disks that comprised our "door" and the "walls", in order to make some definitive statements about the problem.

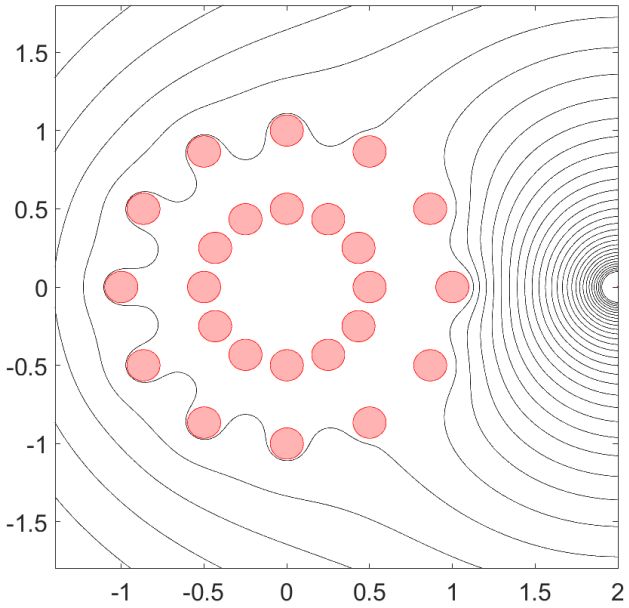

Figure 31: Two circular Faraday cages.

When we are tackling the problem providing maximum shielding for a specific region with a limited amount of material we need to decide on a number of factors. Using our model we observed that it is generally better to use a large number of disks of small radius, rather than a small number with a larger radius. Applying a general methodology to a test scenario we were then able to arrive at an optimal configuration for that specific case with the methodology we used being suitable to tackle a large number of potential situations.

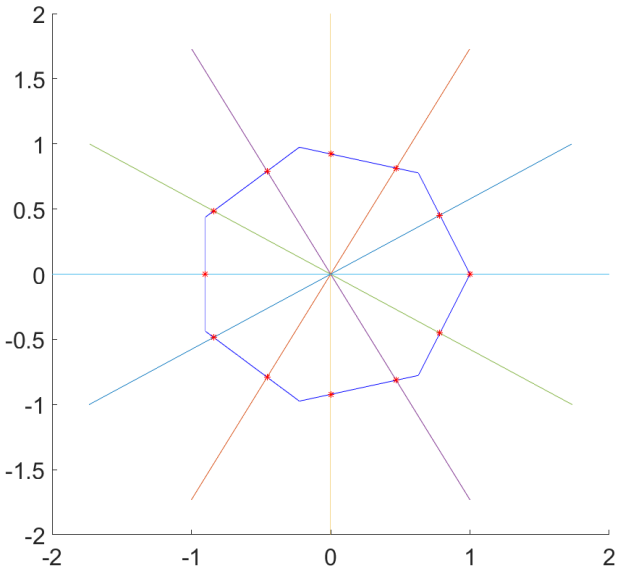

Figure 32: Our new approach visualised, the intersection points marked in red are the points at which we place our disks.

The final specific problem we tackled was that of how to best distribute our disks along the boundary with the goal of minimising the field strength at the center and on average within the boundary. We compared two approaches, our initial approach which involved placing the disks at equally spaced points and a new approach that involved separating the disks by the same angle. By testing both approaches for a variety of different boundary shapes we were able to conclude that this new approach was superior only in the case of a triangular boundary, being extremely similar to the old approach for all other polygons with some minor deviations depending on the number of disks.
These results were not entirely surprising however considering the potential for general improvements to our model was a worthwhile exercise.

Using our results we concluded that by applying this new method it would be possible to slightly improve previously obtained results that involved a triangular boundary in some capacity. We also noted that there is still the possibility that further improvements could be made in regards to how we choose to place the disks that form our Faraday cage, however this should not affect the key points concluded in previous sections and may not be the case.

To find a true optimal manner of placement we would need to consider every possible placement pattern for each number of disks along each potential boundary, which would be a time-consuming process and unlikely to yield significant differences over previously obtained results.

Finally, we briefly covered the possibility of extending our model in various ways as well as the potential real-life applications our model and other similar models might have.

Now that we have completed a review of the conclusions formed over the course of this dissertation all that remains are the appendices. Appendix A will cover the general MATLAB code used whilst Appendix B will cover more specific applications such as the problems covered in section 5.

8 Appendix A

To begin we look at the basic code used in section 3, this code can be split into three sections that we will go through in turn, these are: defining the constraints, solving the problem, and plotting the solution.

```
n = 12; r = 0.1; % number and radius of disks
sides = 360; % number of sides

[x1,y1] = poly(sides);

if sides == 3
    con = 0.64305;
elseif sides == 4
    con = 0.7979;
elseif sides == 360
    con = 0.99999;
else
    con = 1
end

xr1 = x1./con;
yr1 = y1./con;
Area = polyarea(xr1,yr1);
[xr,yr] = divisor(xr1,yr1,n);
c = xr + i.*yr;
```

In the above code we use a function named "poly", this simply creates a regular polygon with the specified number of sides using the roots of unity of a circle and outputs the x and y coordinates of each of the vertices of that polygon in two matrices.

The next section scales the size of the polygon produced appropriately, in this case producing a polygon with surface area equal to π. This is then checked using the "polyarea" function available in MATLAB.

Finally, we use the "divisor" function which divides the resized polygon into n equal parts, we then convert this into a complex number and we have obtained the locations of each of our n disks.

```
rr = r*ones(size(c)); % vector of radii
N = max(0,round(4+.5*log10(r))); % number of terms in expansions
npts = 3*N+2; % number of sample points on circles
circ = exp((1:npts)'*2i*pi/npts); % roots of unity for collocation
z = []; for j = 1:n
z = [z; c(j)+rr(j)*circ]; end % collocation points
A = [0; -ones(size(z))]; % the constant term
zs = 2; % location of the singularity
rhs = [0; -log(abs(z-zs))]; % right-hand side
for j = 1:n
A = [A [1; log(abs(z-c(j)))]]; % the logarithmic terms
for k = 1:N
zck = (z-c(j)).^(-k);
A = [A [0;real(zck)] [0;imag(zck)]]; % the algebraic terms
end
end
X = A\rhs; % solve least-squares problem
e = X(1); X(1) =[]; % constant potential on wires
d = X(1:2*N+1:end); X(1:2*N+1:end) = []; % coeffs of log terms
a = X(1:2:end); b = X(2:2:end); % coeffs of algebraic terms
```

This section of code was provided by the authors of [1]. The basis of this code can be found in an earlier paper by Trefethen in [10] concerning ten digit algorithms, these are algorithms that solve a problem to ten digits of accuracy within five seconds or less whilst being less than one page of code long. The idea being that these algorithms solve the relevant problem efficiently and allow for repeated experimentation without requiring significant amounts of time to run. The specific basis for the code comes from an algorithm devised by Trefethen that approximates Green's function exterior to several disks named "many_disks.m".

This code applies Miklhin's method (as seen in (6) in section 2) to the problem in a manner suitable for MATLAB separating each of the individual terms used to calculate the solution into individual matrices, which are then used to form the solution itself in the section of code below and on the next page.

```
x = linspace(-2,2,1000); y = linspace(-2,2,1000);
[xx,yy] = meshgrid(x,y); zz = xx+1i*yy; uu = log(abs(zz-zs));
for j = 1:n
uu = uu+d(j)*log(abs(zz-c(j)));
for k = 1:N, zck = (zz-c(j)).^(-k); kk = k+(j-1)*N;
uu = uu+a(kk)*real(zck)+b(kk)*imag(zck); end
end
for j = 1:n, uu(abs(zz-c(j))<rr(j)) = NaN; end
z = exp(pi*1i*(-50:50)'/50);
for j = 1:n, disk = c(j)+rr(j)*z; fill(real(disk),imag(disk),[1 .7 .7])
hold on, plot(disk,'-r'), end
contour(xx,yy,uu,-2:.1:1.2), colormap([0 0 0]), axis([-1.4 2 -1.8 2])
axis square, plot(real(zs),imag(zs),'.r')
```

```
[Dx,Dy]=gradient(uu);
g = sqrt(Dx.^2+Dy.^2);
a = g(500,500);
b = a*250;

quiver(xx,yy,Dx*scale_factor,Dy*scale_factor,'AutoScale','on');
```

These two final sections then plot the solution using the matrices obtained in the previous section. This is done by creating a linear space and then producing a contour plot using the solution obtained from Miklhin's method, denoted "uu" in the code. Once we have this plot we can then use the final line of the code to overlay a quiver plot and make the behaviour of the electromagnetic field more apparent.

Lines 1 through 4 in the second of these two sections calculate the gradient of the solution and then the strength of the electromagnetic field at the center of the linear space, which is also the point at the center of the cage. In section 3 we use an alternate methodology to analyse the situation of the optimal boundary shape, namely using the average of the field strength within the cage rather than the field strength at the center. This alternate methodology can be calculated in a simple fashion using MATLAB.

```
Av1 = zeros(length(i),length(j));
for i = 1:1001
    for j = 1:1001
        Av1(i,j) = inpolygon(-1.996+(i*0.004),-1.996+(j*0.004),xr1,yr1);
    end
end

nnz(Av1)
Average = zeros(length(i),length(j));

for i = 1:1001
for j = 1:1001
    if Av1(i,j) == 1
        Average(i,j) = g(i,j)*250;
    else
        Average(i,j) = 0;
end
end
end
Average(isnan(Average))=0;

Final_Average = zeros(1,1);

for i = 1:1001
for j = 1:1001
    Final_Average = Final_Average + Average(i,j);
end
end
Final_Average./nnz(Av1)
```

Here we simply use the "inpolygon" function of MATLAB to determine whether or not each point comprising our linear space is indeed contained within the cage, as the cage is comprised of disks placed along the sides of our initial polygon. If the point is located within the cage then we calculate the field strength at that point and include it in the matrix "Av1" for that coordinate of the linear space which corresponds to a value of i and j which are the rows and columns of Av1, otherwise the corresponding entry of Av1 is set to zero. We then sum the contents of Av1 and divide by the number of non-zero elements of Av1 to obtain our average.

The final piece of general code we need to cover is the code used to produce the tables seen throughout the various sections.

```
sv = [3,4,360];
nv = [1,2,3,4,5,6,7,8,9,10,11,12,13,14,15];
A = zeros(length(i),length(j));
D = zeros(length(i),length(j));

for i = 1:length(nv)
    for j = 1:length(sv)
        n = nv(i);
        s = sv(j);
        [b] = Area_Function_Average(s,n);
        A(i,j) = b;
        D(i,j) = maximum;
    end
end
```

Here we may include values for the number of sides "sv" and the number of disks "nv" as we like, producing a table with the values of nv as the rows and the values of sv as the columns. The current configuration of this code produces the values seen in table 5, with the matrix A giving the average field strength within the cage and the matrix D giving the maximum value of the field strength within the cage. The function "Area_Function_Average" is simply a composition of the previous code covered during this section with the addition of a line calculating the maximum value of the matrix Av1.

Various plots may be created using this basic format, for example plotting each of the columns of the matrix A against "nv" will provide a plot of the shapes given in sv against the number of disks given in "nv".

Now we have covered the general code used we may move onto examples used to tackle more specific problems, for the most part the code used to tackle the specific problems. This will form Appendix B.

9 Appendix B

The code used to tackle specific problems is for the most part simply comprised of logical extensions to the general code provided in Appendix A. The first of these specific problems was the issue of analysing the situation of a two dimensional approximation of a microwave.

```
n1 = 8; % number of disks forming each "wall"
n2 = 4; % number of disks forming the "door"
r = 0.1;

x = [-1 1];
y = [1 1];
[xr1,yr1] = divisor(x,y,n1);
x = [1 1];
y = [1 -1];
[xr2,yr2] = divisor(x,y,n1);
x = [1 -1];
y = [-1 -1];
[xr3,yr3] = divisor(x,y,n1);
x = [-1 -1];
y = [-1 1];
[xr4,yr4] = divisor(x,y,n2);

c1 = xr1 + i*yr1;
c2 = xr2 + i*yr2;
c3 = xr3 + i*yr3;
c4 = xr4 + i*yr4;

[c] = [c1 c2 c3 c4];
c = unique(c);
n = nnz(c);
```

Here we simply create four variables labelled c1 through c4, each of which represents one of the four sides of our microwave. We then simply use the divisor function to find the points at which we should place our disks and then create one matrix containing all of these points. To prevent a point potentially being listed twice we remove any duplicate entries using the "unique" function present in MATLAB and set n to be the number of non-zero entries of our list of points at which we place the disks.

To calculate the average field strength in the area outside of the door we use a very similar approach to one used previously. This section of code can be seen at the top of the following page.

```
xt1 = [-2 -1 -1 -2 -2];
yt1 = [-2 -1 1 2 -2];

for k = 1:1001
    for j = 1:1001
        Av1(k,j) = inpolygon(-1.996+(k*0.004),-1.996+(j*0.004),xt1,yt1);
    end
end
```

The only change is in the polygon used by the inpolygon function, here xt1 and yt1 simply define the area outside of the door, as shown in figure 19. We can use a similar method to calculate the average field strength in any area we desire. It is using this approach that we calculate the average field strength for specific regions as in the second half of section 5.

The final problem tackled in section 5 concerned an alternate methodology for placing the disks that form our cage. The MATLAB code used is quite simple however it does require some explanation.

```
divisions = 6;
n = divisions.*2; r = 0.1;
sides = 360;
alpha_zero = pi/divisions;
L = 2;
```

Here we simply define the relevant variables we will be using. The two new variables of concern are "alpha_zero" and "L", "alpha_zero" is simply the angle between each of the disks measured in radians, which in this case is 30°s, whilst "L" is the length of the line. The exact value of "L" is unimportant, the only requirement being that it is long enough to interest with the boundary polygon as shown in figure 24 on page 28. The majority of the rest of the code used is the same as our general model for the most part, as such we will only be covering the new additions.

```
u = [0];
v = [0];
A = zeros(divisions,2);

for k = 1:divisions
     alpha = k.*alpha_zero;
     xa(k) = u+(L*cos(alpha));
     ya(k) = v+(L*sin(alpha));
     xa(abs(xa)<0.01)=0;
     ya(abs(ya)<0.01)=0;
     hold on
     plot([-xa(k) xa(k)],[-ya(k) ya(k)]);
     A(k,1) = xa(1,k);
     A(k,2) = ya(1,k);
end
```

```
A1 = zeros(1,divisions);
A2 = zeros(1,divisions);

for j = 1:divisions
    [x,y] = intersections(xr1,yr1,[-xa(:,j) xa(:,j)],[-ya(:,j) ya(:,j)])
       ;
    plot(x(1,:),y(1,:),'r*');
    plot(x(2,:),y(2,:),'r*');
    A1(1,j) = x(1,:) + i.*y(1,:);
    A2(1,j) = x(2,:) + i.*y(2,:);
end

c = horzcat(A1,A2);
```

This code can be split into two main sections, the first of which is located at the bottom of the previous page and the second at the top of this one. The first section simply generates the endpoints of our lines and places them in matrix A. The second then takes these lines and calculates the points at which they intersect with our polygon using the "intersections" function. The end result is a list of points at which we may place our disks which results in a distribution where every disks is separated from its neighbours by the desired angle. This allows us to produce results for any angle we desire and for any regular polygon, with it being quite easy to extend the model to a boundary of any shape with little effort needed.

References

[1] S.J. Chapman, D.P. Hewett, and L.N. Trefethen, "Mathematics of the Faraday Cage".

[2] M. Faraday, Experimental Researches in Electricity, v. 1, reprinted from Philosophical Transactions of 18311838, Richard and John Edward Taylor, London, 1839 (paragraph 1174, p.366).

[3] R. Feynman, R. B. Leighton, and M. Sands, The Feynman Lectures on Physics, v. 2: Mainly Electromagnetism and Matter, Addison-Wesley, 1964.

[4] L. N. Trefethen, Ten digit algorithms, Oxford technical report.

[5] Yue Qi, Various, Switching Vertical to Horizontal Graphene Growth Using Faraday CageAssisted PECVD Approach for HighPerformance Transparent Heating Device, 10th January 2018, https://doi.org/10.1002/adma.201704839.

[6] A 3D Faraday Shield for Interdigitated Dielectrometry Sensors and Its Effect on Capacitance, Alex Risos.

[7] Shielding, 2018, Appliance Design. Jan2018, Vol. 66 Issue 1, p15-17. 3p.

[8] A Mobile Phone Faraday Cage, M M J French, Physics Education Vol.46, 2011.

[9] D. Hewett and I. Hewett, Homogenised Boundary Conditions and Resonance Effects in Faraday Cages, 4th May 2016, http://rspa.royalsocietypublishing.org/content/472/2189/20160062

[10] Rauno Pkknen, Various, Possibilities to decrease the extremely low-frequency electric field exposure with a Faraday cage under a 400 kV power line, 8th August 2016, https://ieeexplore-ieee-org.chain.kent.ac.uk/document/7734884/